Zierenberg, R.A., Fouquet, Y., Miller, D.J., and Normark, W.R. (Eds.)
Proceedings of the Ocean Drilling Program, Scientific Results Volume 169

10. Overview of Ocean Drilling Program Leg 169: Sedimented Ridges II[1]

Robert A. Zierenberg[2] and D. Jay Miller[3]

ABSTRACT

Leg 169 of the Ocean Drilling Program built upon the success of Leg 139 in investigating the geological, geophysical, geochemical, and biological processes at sediment-covered spreading centers in the northeast Pacific Ocean. The primary scientific objective of Leg 169 was to investigate the genesis of massive sulfide deposits by drilling two deposits at different stages of maturity: Middle Valley at the northern end of the Juan de Fuca Ridge and Escanaba Trough at the southern end of the Gorda Ridge. The four primary topics of investigation during this leg were (1) the mechanism of formation of massive sulfide deposits at sediment-covered ridges, (2) the tectonics of sedimented rifts and controls on fluid flow, (3) the sedimentation history and diagenesis at sedimented rifts, and (4) the extent and importance of microbial activity in these environments.

Postcruise research of the shipboard scientific party submitted to the *Scientific Results* volume for Leg 169 includes investigations into porewater chemistry; sulfide and clay mineral petrology and geochemistry; the physical properties of basalt, sediments, and sulfides; the structural framework of the feeder zone of a seafloor hydrothermal system; and estimates of the biomass and microbiological diversity attending the growth and evolution of a sediment-hosted massive sulfide deposit. Manuscripts accepted for publication elsewhere at the time of submission of this synopsis include a study of deep-sea sedimentation resulting from cataclysmic floods off the west coast of North America, porewater chemistry and systematics, and metal sources in the massive sulfides.

Postcruise analyses of sulfide mineralization and wall rock alteration were still in progress at the time this overview was written, but several

[1]Zierenberg, R.A., and Miller, D.J., 2000. Overview of Ocean Drilling Program Leg 169: Sedimented Ridges II. *In* Zierenberg, R.A., Fouquet, Y., Miller, D.J., and Normark, W.R. (Eds.), *Proc. ODP, Sci. Results,* 169, 1–39. [Online]. Available from World Wide Web: <http://www-odp.tamu.edu/publications/169_SR/VOLUME/CHAPTERS/SR169_10.PDF>. [Cited YYYY-MM-DD]
[2]Department of Geology, University of California, Davis, One Shields Avenue, Davis CA 95161-8605, USA. **zierenberg@geology.ucdavis.edu**
[3]Ocean Drilling Program, Texas A&M University, 1000 Discovery Drive, College Station TX 77845-9547, USA.

Date of initial receipt: 18 April 2000
Date of acceptance: 5 May 2000
Date of publication: 31 August 2000
Ms 169SR-119

preliminary conclusions can be drawn from the available data. Mineralization at the Middle Valley site was the result of a structurally focused, long-lived hydrothermal system. This resulted in deposition of at least 100 m of massive sulfide at the Bent Hill deposit and the formation of three stratigraphically stacked massive sulfide lenses at the ODP Mound site. Both deposits are underlain by extensive Cu-rich feeder zone mineralization. A subseafloor silicification zone formed a caprock that forced hydrothermal fluid flow into permeable sandy horizons where high-grade copper ore formed by replacement of sediment. Fracturing of the silicified caprock near the time when the intrusion of basaltic magma uplifted Bent Hill may have been responsible for a second pulse of hydrothermal activity at the Bent Hill Massive Sulfide deposit. Drilling through the silicified zone reinitiated hydrothermal activity at both the Bent Hill and ODP Mound deposits.

Drilling at Escanaba Trough revealed extremely high sedimentation rates related to breaching of glacial lakes in the Columbia River basin. The sheeted sill style of oceanic crustal development that characterizes the central rift in Middle Valley is generally lacking at Escanaba Trough. Sulfide deposition at Escanaba Trough occurred due to a recent hydrothermal pulse that led to widespread diffuse venting of high temperature hydrothermal fluids. The hydrothermal fluids reacted extensively with the sediments, enriching the massive sulfide deposits in sediment-derived metals. Pore fluids include both high-salinity brines and low-salinity fluids formed by phase separation. This short but intense hydrothermal episode appeared to lack strong structurally controlled fluid flow paths. Intense hydrothermal alteration and stringer zone mineralization were not encountered beneath massive sulfide at Escanaba Trough.

SCIENTIFIC RESULTS

Introduction

Eruption of volcanic rocks at midocean ridges is the major mechanism by which heat is lost from the interior of the Earth. Approximately one-third of the heat delivered by the emplacement of magma at the spreading centers is removed by circulation of cold seawater through the hot volcanic rocks that make up the oceanic crust. Seawater interacts with the volcanic rocks at temperatures near 400°C resulting in substantial chemical exchange between seawater and the igneous basement. The flux of elements between seawater and the oceanic crust makes an important contribution to buffering the composition of some elements in seawater (Edmond and Von Damm, 1983; Elderfield and Schultz, 1996). Discharge of hydrothermal fluids onto the seafloor also results in the deposition of metallic sulfides at hydrothermal vents, forming deposits similar to volcanic-associated massive sulfide (VMS) ore deposits (Hannington et al., 1995).

Basaltic rocks are exposed directly at the seafloor over nearly the entire length of the midocean ridge system, but locally, where ridges are near the continental margins, the spreading centers can be covered by sediment. Hydrothermal circulation is still an important process at sediment-covered spreading centers, but the presence of a low permeability sediment blanket over the more permeable volcanic basement changes the fluid and heat flux of the hydrothermal system (Davis and Fisher, 1994).

Leg 169 was the second leg of a planned two-leg program to investigate the geological, geophysical, geochemical, and biological processes at sediment-covered spreading centers in the northeast Pacific Ocean (Fig. F1). Building on the highly successful Leg 139 drilling (Davis, Mottl, Fisher, et al., 1992), our primary goal was to investigate the genesis of massive sulfide deposits by drilling two deposits at different stages of maturity: Middle Valley at the northern end of the Juan de Fuca Ridge and Escanaba Trough at the southern end of the Gorda Ridge. If our objectives were achieved, we expected Middle Valley to reveal details about a mature system, whereas the Escanaba Trough deposits were thought to be representative of the genesis of a massive sulfide-bearing seafloor hydrothermal system. The four primary topics investigated during this leg were (1) the mechanism of formation of massive sulfide deposits at sediment-covered ridges, (2) the tectonics of sedimented rifts and controls on fluid flow, (3) the sedimentation history and diagenesis at sedimented rifts, and (4) the extent and importance of microbial activity in these environments.

This report reviews the geological setting of the sites investigated during Leg 169 and provides an overview of the scientific results from shipboard observation and postcruise studies on samples recovered by drilling. At the time this report was written, much of the postcruise research was still in progress, so this overview should be considered to be preliminary.

F1. Spreading centers at Middle Valley and Escanaba Trough, p. 29.

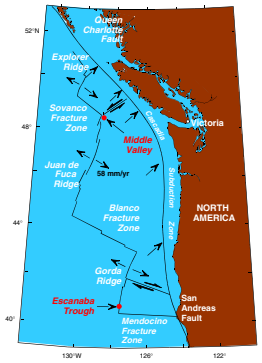

Middle Valley: Geology of the Hydrothermal Field

Middle Valley is a medium-rate spreading center (58 mm/yr) that forms one leg of a ridge-transform-transform unstable triple junction with the Sovanco Fracture Zone and the Nootka fault (Davis and Villinger, 1992). The proximity of Middle Valley to the cold Explorer plate results in a reduced magma supply and a slow-spreading ridge morphology with a deep and wide axial trough. Current magmatic activity is mostly confined to the adjacent West Valley spreading center, indicative of a recent jump in the location of the plate boundary. Proximity of the Middle Valley spreading center to an abundant supply of terrigenous sediment during the Pleistocene sea-level lowstand has resulted in burial of the spreading center by 200 to >1000 m of turbiditic and hemipelagic sediment, with sediment thickness increasing to the north. Two areas of hydrothermal activity, separated by ~4 km, were initially drilled during Leg 139 and were further investigated during Leg 169. The Dead Dog vent field (Sites 858 and 1036) is the area of most active venting in Middle Valley (Fig. F2). The Bent Hill area (Site 856 and 1035) at present has limited hydrothermal activity, but was formerly the site of vigorous high-temperature hydrothermal discharge. Two large mounds of massive sulfide were investigated by drilling in the Bent Hill area.

F2. Bathymetry of Middle Valley including Dead Dog vent field and Bent Hill, p. 30.

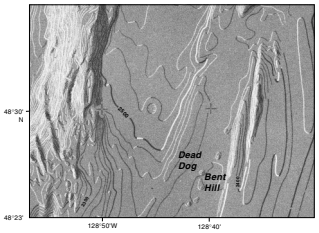

F3. Map of Bent Hill, p. 31.

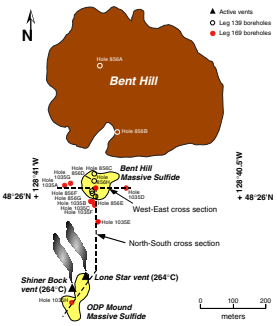

Bent Hill

Bent Hill is one of a string of small mounds that runs parallel to the eastern rift-bounding normal fault scarp. These features lie close to an inferred normal fault that appears to offset basement reflectors, but near-surface sediment layering imaged in seismic reflection profiles appears to be continuous across this fault. Bent Hill is a roughly circular feature 400 m in diameter that has been recently uplifted ~50 m (Fig. F3). It is bounded on the west by a steep scarp that parallels the rift-

bounding faults and exposes semiconsolidated turbiditic sediment. Bright, reverse polarity seismic reflections that are limited in extent to the area under Bent Hill are interpreted to be generated at the interface between the base of basaltic sills and the underlying sediments (Rohr and Schmidt, 1994).

The 35-m-high Bent Hill Massive Sulfide (BHMS) deposit is located 100 m south of Bent Hill. A second twin-peaked massive sulfide deposit (ODP Mound) is located ~330 m farther south. These mounds are aligned parallel to the north-south-trending scarp that constitutes the western side of Bent Hill. The BHMS deposit is extensively weathered to Fe oxyhydroxides and partially buried by sediment. During Leg 139, Hole 856H penetrated 94 m of massive sulfide before the hole had to be abandoned because of an inflow of heavy sulfide sand from the upper weathered section of the borehole wall. A strong magnetic anomaly across this mound, related to the occurrence of magnetite, had been modeled to suggest that mineralization continued at least another 30 m below the level drilled and possibly much deeper (Tivey, 1994).

The morphology, degree of oxidation, and the lack of sediment cover on the mound south of the BHMS deposit indicate that these deposits are younger than the Bent Hill deposit. A local heat-flow anomaly occurs around the BHMS because of the high thermal conductivity of the massive sulfide body (Fisher et al., 1997). A more pronounced heat-flow high occurs at ODP Mound (Davis and Villinger, 1992; Fisher et al., 1997; Stein et al., 1998). Prior to drilling, a single 264°C hydrothermal vent had been located on the northern mound. The composition of the vent fluid is generally similar to those from the Dead Dog vent field, but this vent has lower salinity and only half as much dissolved Ca (Butterfield et al., 1994). Hole 1035H was spudded ~30 m away from a second area of hydrothermal venting that occurs near the saddle of ODP Mound. This area of hydrothermal venting was observed during the camera survey to spud Hole 1035H and was subsequently visited and sampled using the *Alvin* submersible. The maximum vent temperature measured was also 264°C (R. Zierenberg, unpubl. data).

Dead Dog Vent Field

The principal center of hydrothermal activity in Middle Valley is the Dead Dog vent field. Contoured heat-flow values show a concentric high (Davis and Villinger, 1992; Fisher et al., 1997; Stein et al., 1998), which is coincident with a sidescan acoustic anomaly (Fig. **F4**) that outlines the 800-m-long and 400-m-wide vent field. Sediment thickness over the fault block in the area surrounding the vent field is ~450 m and overlies a sill-sediment complex that forms the transition to oceanic crust (Davis, Mottl, Fisher, et al., 1992). Hard acoustic reflectors recorded immediately beneath the vent field during site surveys were determined by drilling during Leg 139 to be the top of a volcanic edifice at only 250 m depth. The presence of more permeable volcanic basement penetrating up into the sediment cover acts as a conduit that focuses flow of hydrothermal fluid to the seafloor (Davis and Fisher, 1994). The vent field contains at least 20 active vents with fluid temperatures ranging up to 276°C (Ames et al., 1993). Active vents are predominantly on top of 5- to 15-m-high sediment-covered mounds a few tens of meters in diameter. Available data from piston cores and Hole 858B suggested that subsurface deposition of anhydrite, Mg-rich smectite, and sulfide minerals contribute to the growth of the mounds. Because the high-temperature hydrothermal fluid is strongly depleted in both

F4. Map of Dead Dog vent field, p. 32.

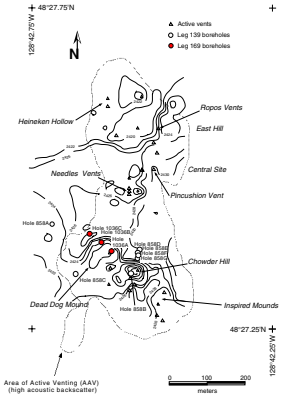

Mg and SO_4, the abundance of these minerals in the subsurface requires that cold seawater (with abundant Mg and SO_4) is drawn into the subsurface by the vigorous upflow at the active vent sites. In situ pore-pressure measurements (Schultheiss, 1997) and hydrologic modeling (Stein and Fisher, in press) indicate that seawater is being recharged into the uppermost part of the hydrothermal system. Modeling of pore-fluid compositional gradients in piston cores collected from the Dead Dog vent field also indicates local drawdown of seawater into the sediments (Glenn, 1998).

A major step toward the establishment of seafloor observatories was taken during Leg 139 by instrumentation of two sealed boreholes in the Middle Valley hydrothermal field using a circulation obviation retrofit kit (CORK) system (Davis and Becker, 1994a). The thermistor strings in these sealed boreholes eventually failed because of high formation temperatures. Part of the science plan for Leg 169 was to reinstrument these sealed boreholes to allow active experimentation on induced seismicity in a seafloor hydrothermal system and hole-to-hole hydrologic experimentation designed to constrain the physical and hydrologic properties that control hydrothermal flow on the scale of an entire vent field. An additional objective of Leg 169 was sampling of hydrothermal fluids from these sealed boreholes.

Escanaba Trough: Geology of the Hydrothermal Field

The Gorda Ridge spreading center is located offshore of Oregon and northern California and is bounded by the Mendocino Fracture Zone on the south and the Blanco Fracture Zone on the north (Fig. F1). A small offset in the spreading axis at 41°40´N latitude marks the northern boundary of Escanaba Trough, which forms the southernmost part of Gorda Ridge. Escanaba Trough is opening at a total rate of ~24 mm/yr and has a morphology consistent with its slow-spreading rate. The axial valley, which is at a depth of 3300 m, increases in width from ~5 km at the north end to >15 km near the intersection with the Mendocino Fracture Zone.

Escanaba Trough Reference Site

South of 41°17′(S)N latitude, the axial valley of Escanaba Trough is filled with several hundred meters (Fig. F5) of turbiditic sediment. The sedimentary cover thickens southward and is a kilometer or more in thickness near the Mendocino Fracture Zone. Turbiditic sediment enters the trough at the southern end and is channeled northward by the axial valley walls (Vallier et al., 1973; Normark et al., 1994; Brunner et al., 1999). Sedimentation was relatively rapid (up to 10 m/1000 yr) during sea-level lowstands in the Pleistocene, and the entire sediment fill of the trough probably was deposited within the last 100 k.y. (Normark et al., 1994; Davis and Becker, 1994b; Brunner et al., 1999). A reference hole through this sedimentary package and into basaltic basement was drilled to provide background information to evaluate the sedimentary and thermal history in an area away from the hydrothermal upflow zone.

F5. Map of Escanaba Trough, p. 33.

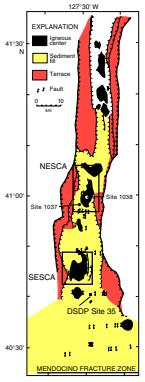

Central Hill Area

Seismic reflection surveys show that the floor of Escanaba Trough is generally a smooth, flat plain underlain by continuous and relatively

undisturbed turbidites. However, local areas along the axis of spreading have irregular seafloor topography characterized by circular hills 0.5 to 1.2 km in diameter that are uplifted 50 to 120 m above the surrounding seafloor. The areas of sediment disruption are sites of recent axial-rift igneous activity. Geologic and geophysical evidence suggests that axial-rift igneous activity at these sites is manifested by the intrusion of dikes, sills, and laccoliths into the sediment with less abundant volcanic flows (Morton and Fox, 1994; Zierenberg et al., 1993, 1994). Sulfide mineralization has been sampled by dredging, sediment coring, or submersible at four igneous centers within the sediment-covered part of Escanaba Trough. The dominant morphologic feature in the area of operations for Leg 169 was Central Hill (Fig. F6).

The western, sediment-covered part of Central Hill contains the most extensive sulfide deposits observed in Escanaba Trough. The massive sulfide deposits on the west and southeast flanks of Central Hill are actively venting hydrothermal fluid, and the area on the northern flank shows indications of very recent hydrothermal activity, suggesting that these deposits are all part of the same hydrothermal system. The best explored and most hydrothermally active area of sulfide mineralization on Central Hill extends west and north from the northern end of the sediment-covered hilltop. On the northern flank of the hill, massive sulfide extends >270 m from north to south and >100 m from east to west, but the western edge of the deposit has not been defined with certainty. All of the active hydrothermal vents are in an area with abundant sulfide mounds along the northwestern flank of the hill. The major element composition of the end-member hydrothermal fluid of two actively discharging vents 275 m apart is identical (Campbell et al., 1994), a result that is consistent with the hypothesis that this large mineralized area is a single hydrothermal system hydrologically interconnected at depth. The highest vent-fluid temperature measured in this field is 217°C, and the hydrothermal fluids venting in 1988 had a chloride content ~24% higher than bottom seawater (Campbell et al., 1994).

Sulfide samples collected at the surface of the deposit are predominantly pyrrhotite with variable amounts of sphalerite, isocubanite, and chalcopyrite, and minor galena, lollingite, arsenopyrite, and boulangerite. Sulfate is present as barite crusts and chimneys on massive sulfide and intergrown barite-anhydrite in active vents. When compared to Middle Valley, the abundance of barite and enrichment of metals such as lead, arsenic, antimony, and bismuth indicate extensive contribution from sediment source rocks (Koski et al., 1994). Lead isotope ratios of massive sulfide indicate that most of the lead in the deposits is derived from leaching of sediments (Zierenberg et al., 1993). Precious metals are significantly enriched relative to Middle Valley massive sulfide (Koski et al., 1994). Sediment alteration associated with formation of massive sulfides is dominated by Mg-rich chlorite, talc, or Mg-rich smectite (Zierenberg et al. 1994).

F6. Map of Central Hill, p. 34.

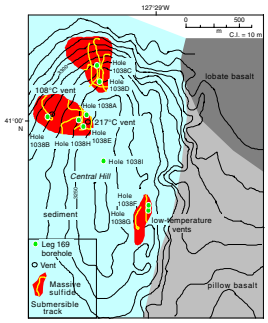

RESULTS FROM LEG 169

Middle Valley

Massive Sulfide Deposits in the Bent Hill Area

Eight holes were drilled in the vicinity of the BHMS deposit to assess the thickness and lateral extent of the massive sulfide deposit and to determine the nature of the hydrothermal feeder zone in the sediments and basalt underlying the deposit. The BHMS deposit is the result of a complex interaction between hemipelagic and turbiditic sedimentation, igneous activity, and hydrothermal circulation. The deposit includes iron- and zinc-rich massive and semimassive sulfides, a well-developed feeder zone characterized by crosscutting copper-rich veins and sulfide impregnation of sediment, and a deep stratiform zone of copper-rich mineralization that was deposited in a sandy unit that was an important conduit for lateral fluid flow.

Hole 856H was drilled on the topographic high point of the BHMS deposit and is thought to cut through the thickest portion of the sulfide deposit. This hole can be considered as a reference section for comparison of the vertical and lateral variations in the sulfide deposit and associated host rocks (Fig. F7). From top to bottom, the hole penetrated successively: massive sulfide (0–103.6 mbsf), a sulfide feeder zone (103.6–210.6 mbsf), interbedded turbidite and pelagic sediments (210.6–431.7 mbsf), a 39.4 m interval of basaltic sills and sediment, and 28.9 m of basaltic flows.

Most of the massive sulfide unit was drilled during Leg 139 and the material recovered is described in Davis, Mottl, Fisher, et al., (1992) and Mottl, Davis, Fisher, and Slack (1994). The upper 75 m of the massive sulfide shows a variable extent of recrystallization of pyrrhotite to pyrite including significant intervals of massive pyrite with only trace amounts of other sulfide minerals. The lowermost 25 m of massive sulfide is predominantly pyrrhotite-rich massive sulfide with 1%–5% interstitial sphalerite/wurtzite and intermediate solid solution (ISS), most of which has unmixed into isocubanite host grains with fine chalcopyrite exsolution lamellae. Only minor veining and recrystallization of pyrrhotite to pyrite and magnetite is present in this zone, and the lowermost samples of massive sulfide that were recovered contain significantly more isocubanite and chalcopyrite.

The underlying feeder zone is divided into three subunits. The uppermost unit is sulfide-veined siltstone and mudstone (103.6–152.9 mbsf) where the major sulfides are isocubanite, chalcopyrite, and pyrrhotite (Lawrie and Miller, Chap. 5, this volume; Marquez and Nehlig, Chap. 9, this volume) found in subvertical, anastomosing veins. Below this interval, sediments have only minor disseminated and vein-controlled sulfide (152.9–201 mbsf). From 210.6 to 249.0 mbsf is a sulfide-banded sandstone, highly enriched in copper relative to the overlying mineralization, that has been designated the Deep Copper Zone (DCZ). The contact between the DCZ and the underlying sediment is extremely sharp.

The sediment underlying the feeder zone is nonmineralized to slightly mineralized turbidites. Based on hydrothermal alteration and color, three intervals were defined on board ship. The uppermost subunit (210.6–249.0 mbsf) is relatively unaltered sediment composed of gray, fine-sand turbidites. Below this is an interval of greenish gray siltstone and mudstone (249.0–345.5 mbsf) with abundant chlorite. The

F7. North-south cross section of the BHMS deposit and ODP Mound, p. 35.

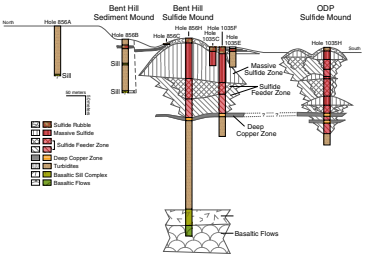

lowermost sedimentary subunit is again predominantly gray fine sandstone turbidites (3245.5–431.7 mbsf).

The base of the sedimentary section (431.7–471.3 mbsf) has been intruded by five basaltic sills from 1 to >5 m thick. The igneous rocks are variably altered and crosscut by veins containing quartz, chalcopyrite, pyrrhotite, sphalerite, calcite, and epidote. These sills are intercalated with indurated and hydrothermally metamorphosed sediment, and this unit is interpreted to represent transitional oceanic crust similar to, but much thinner than, the sill-sediment complex penetrated by Hole 857A during Leg 139 (Davis, Mottl, Fisher, et al., 1992). Thirty meters of basaltic flows (471.1–500 mbsf) underlying the sill sediment complex was drilled. These flows are similar in mineralogy and alteration to the sills. If these flows represent the top of a standard section of oceanic crusts, then it appears that the Bent Hill deposit formed near the transition from normal oceanic crust to sedimented-rift type crust (Currie and Davis, 1994). However, the hydrothermal activity was clearly later than the formation of the igneous basement, as sufficient time passed for the accumulation of 350 m of turbidites that formed a thermal blanket and hydrologic seal over the more permeable oceanic crust.

The surface of the sulfide deposit exposed at the seafloor is characterized by gossanous iron-oxide fragments, clasts of pyrrhotite-rich massive sulfide, and vuggy pyritic massive sulfide. A carapace of brecciated and clastic sulfide, including oxidized material, overlies the massive sulfide in most of the drill holes. Some of this material seems to represent material formed by oxidative weathering and disaggregation of massive sulfide exposed at the seafloor. Goodfellow et al. (1993) interpreted some sulfide fragments recovered in piston cores from the top BHMS deposit to represent detritus from collapsed sulfide chimneys that have not undergone the extensive hydrothermal recrystallization that characterizes the bulk of the deposit.

Surprisingly, although the massive sulfide mound must have extended to 100 m above the turbidite-covered seafloor, there is essentially no clastic sulfide deposited with the bulk of the turbidites that bury the flanks of the mound. A unit of interbedded clastic sulfide and sediment was recovered in the uppermost 10 m of sediment in holes to the east, west, and south of the sulfide mound (Fouquet, Zierenberg, Miller, et al., 1998). Similar material was recovered from the uplifted flank of Bent Hill in Hole 856B (18–24 mbsf; Rigsby et al., 1994), but the occurrence of this interval in a zone of slumping makes determination of the original stratigraphic depth uncertain (Mottl et al., 1994). The clastic sulfides are predominately sulfide-rich turbidites composed of sand- to clay-sized sulfide grains with blue-green clay similar to that observed in the weathered residue formed by the dissolution of collapsed anhydrite-rich hydrothermal chimneys from the active vent fields (Turner et al., 1993).

The hydrothermal recrystallization of the massive sulfide, the presence of some intercalated sulfide and sediment at the top of the deposit, and the distribution and mineralogy of clastic sulfide around the edges of the mound suggest that a second episode of hydrothermal venting occurred more recently at the Bent Hill deposit. Larger massive sulfide clasts in the turbidites are composed predominantly of interlocking bladed pyrrhotite with pyrite, sphalerite, and chalcopyrite (Goodfellow and Franklin, 1993; Fouquet, Zierenberg, Miller, et al., 1998). Fragments of vuggy or massive pyrite similar to that which is present throughout much of the recrystallized portions of the massive sulfide mound have not been recognized in the clastic sulfide turbid-

ites. This suggests that this interval represents collapsed chimney debris shed from the mound rather than redeposited fragments of clastic sulfide derived by erosion of the mound. Clastic sulfides have higher contents of Pb, As, Sb, and Se than massive sulfide from the Bent Hill deposit (Goodfellow and Franklin, 1993; Fouquet, Zierenberg, Miller, et al., 1998) indicating an increased contribution of metals leached from sediment during this hydrothermal stage. Lead in the clastic sulfides has a higher ratio of radiogenic isotopes compared with the massive sulfide zones (Bjerkgård, et al., in press). Although analyses are limited at present, the base metal ratios of this material are similar to material from the presently active vents in Middle Valley (Ames et al., 1993). This second pulse of hydrothermal flow may have been responsible for the extensive recrystallization of massive sulfide in the hydrothermal mound as well as the abundant anhydrite that fills pore space in many of the massive sulfide samples from the flanks of the mound. The presence of slumped sediment immediately below the intervals of clastic sulfide is consistent with an episode of faulting or intrusion of basalt beneath Bent Hill, either of which could have reinitiated hydrothermal discharge by breaching the silicified caprock that presently forms a hydrologic seal on this hydrothermal system, as discussed below.

The massive sulfide zone in the BHMS deposit is a large mound with relatively steep flanks and a near-horizontal base (Fig. F7). The base of the massive sulfide lens is interpreted to represent a time horizon marking the onset of vigorous hydrothermal venting at this site (Zierenberg et al., 1998). Most of the massive sulfide was deposited above the sediment/water interface and the rate of deposition was faster than the rate of sedimentation such that little to no sediment was incorporated into the core of the deposit. The mound eventually built ~100 m above the surrounding seafloor. The thickness of massive sulfide changes abruptly between Hole 1035G, located 68 m west of Hole 856H, and 9 m further west at Hole 1035A, suggesting that these holes are near the western edge of the sulfide deposit, although thinning caused by normal faulting and slumping is possible. Hole 1035D, drilled 75 m east of Hole 856H, penetrated in excess of 40 m of massive and semimassive sulfide, so the eastern edge of the deposit remains undefined. In contrast to the relatively low-grade pyritic massive sulfide recovered from Holes 1035A and 1035G, mineralization in Hole 1035D resembles the upper portions of the deposit recovered in Hole 856H and has variable contents of pyrrhotite, pyrite, magnetite, sphalerite, and isocubanite-chalcopyrite. Compared to the central part of the mound, this lateral extension is depleted in high-temperature minerals such as chalcopyrite, isocubanite, and pyrrhotite. Authigenic anhydrite and pyrite are common as veins, nodules, and disseminated crystals. Hole 1035F was drilled at the base of the BHMS deposit 60 m south of Hole 856H and penetrated at least 80 m of massive to semimassive sulfide, including massive to semimassive pyrrhotite and pyrite with altered sediment (14.5–22.5 mbsf), vuggy massive pyrite with minor chalcopyrite, anhydrite, and sphalerite (22.5 77 mbsf), and massive to semimassive, fine-grained pyrrhotite and pyrite with white clayey altered mudstone (77–89.9 mbsf). Altered sedimentary intervals intercalated with the sulfide are located toward the edges of the sulfide mound, especially near the lower or upper contacts of massive sulfide with sediment. Local veining and replacement of sediment are indications of subsurface sulfide mineralization.

The lack of interbedded sediment throughout much of the deposit indicates that the bulk of the massive sulfide at Bent Hill formed in a single episode of sulfide mound building that was rapid relative to the

rate of turbidite sedimentation. Hydrothermal recrystallization of early deposited sulfide minerals is very common in the massive sulfide. The primary hydrothermal precipitates were dominantly pyrrhotite with less abundant high temperature Cu-Fe sulfide that have bulk-grain compositions within the field for ISS, and sphalerite and/or wurtzite (Davis, Mottl, Fisher, et al., 1992; Krasnov et al., 1994; Duckworth et al., 1994; Fouquet, Zierenberg, Miller, et al., 1998; Lawrie and Miller, **Chap. 5,** this volume). Much of the deposit has been recrystallized to pyrite ± magnetite, and base metal sulfides show textural evidence for dissolution in some parts of the deposit and late-stage veining and replacement in other horizons. This process is generally referred to as zone refining and has resulted in intervals of higher grade base-metal mineralization, especially toward the top and flanks of the deposit (Davis, Mottl, Fisher, et al., 1992; Fouquet, Zierenberg, Miller, et al., 1998).

We estimate that the Bent Hill Massive Sulfide lens is ~200 m across at its base along the east to west drill hole transect. The north to south dimensions of the deposit are constrained by the lack of massive sulfide in Hole 856B, drilled 153 m north of Hole 856H, and by Hole 1035F, drilled 60 m south of Hole 856H, which penetrated >80 m of massive sulfide. A conservative estimate of the size of the massive sulfide mound can be obtained by assuming the lens has the shape of a half sphere with a diameter of 200 m. Using the measured density of 4.2 g/cm^3 (Fouquet, Zierenberg, Miller, et al., 1998), the massive sulfide lens has a minimum size of 8.8×10^6 t (Zierenberg, et al., 1998.). This estimate does not include a significant portion of the mineralization that was deposited below the seafloor in the feeder zone, which is discussed below.

One of the major accomplishments of Leg 169 was the first successful penetration through the feeder zone mineralization underlying a seafloor massive sulfide deposit. This zone represents the pathway for the hydrothermal fluids that deposited the massive sulfide. Feeder zone mineralization associated with similar ancient massive sulfide deposits on land often represent a significant portion of the economic reserves of deposits. In contrast to some ancient massive sulfide deposits, the feeder zone mineralization under the BHMS deposit has not been metamorphosed or deformed.

Feeder zone mineralization is best represented in core from Hole 856H (100–210 mbsf), which recovered a spectacularly developed sulfide feeder zone (Fig. **F8**). The feeder zone has been subdivided into three subunits based on the style and intensity of mineralization and alteration (Fouquet, Zierenberg, Miller, et al., 1998; Marquez and Nehlig, **Chap. 9,** this volume). The upper 45 m of the feeder zone is intensely veined at the top with vein density decreasing downcore. Veins range from at least 8 cm to <1 mm; the thickest veins near the top of this interval typically show crack seal textures indicative of multiple episodes of vein opening because of fluid overpressure, followed by vein-filling mineral precipitation (Fig. **F9**). The veins are predominantly subvertical in the upper section of the feeder zone. Intergrown isocubanite-chalcopyrite and pyrrhotite are the predominant vein-filling minerals with minor to trace amounts of sphalerite and late-stage marcasite or pyrite ± magnetite replacing pyrrhotite. Nonsulfide minerals are not abundant and include chlorite and quartz, which generally are present along the vein margins. The altered turbiditic sediment that hosts the veins is altered to chlorite, quartz, and fine-grained rutile and titanite (Lackschewitz et al., 2000).

F8. Sediment from the feeder zone beneath the BHMS deposit, p. 36.

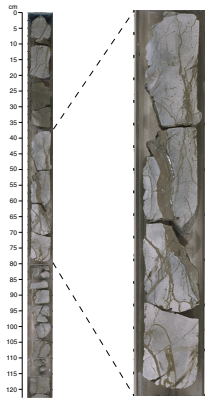

F9. Coalescing of thin veins and crack-seal formation, p. 37.

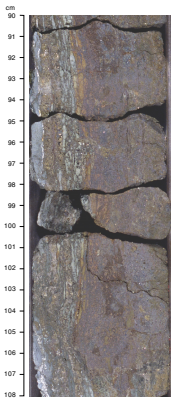

The interval from ~145 to 200 mbsf is less intensely veined. Vein thickness averages ~1 mm. The relative proportion of subhorizontal veins and bedding parallel disseminated sulfide increases progressively down the core. Many subvertical veins branch off into subhorizontal sulfide impregnations in more permeable horizons.

Core recovered below ~200 mbsf is again intensely mineralized, containing up to 50 vol% sulfide minerals (Deep Copper Zone). Sulfide mineralization occurs as impregnations and replacement of the host sediments and is strongly controlled by variation in the original sedimentary textures. Much of the mineralization is developed in medium- to coarse-grained, locally crossbedded, turbiditic sand. The sulfide mineralization locally preserves the original sedimentary structures (Fig. F10). Electron microprobe analyses show that the dominant sulfide mineral is ISS, which typically has unmixed to host grains with a composition near stoichiometric isocubanite (Fe:Cu 2.0–2.1) containing coarse exsolution lamellae of very iron-rich chalcopyrite (Fe:Cu 1.2) (R. Zierenberg, unpubl. data). Pyrrhotite is present but is much less abundant than in the overlying veins; other sulfide minerals are present in only trace amounts. A representative sample of high-grade mineralization from this zone contains 16.1 wt% Cu (Fouquet, Zierenberg, Miller, et al., 1998). The host rock is completely altered to a silvery gray chlorite. Hydrothermal quartz and rutile are present as clear, euhedral crystals disseminated in the chlorite matrix.

F10. Sulfide-banded, cross-laminated sandstone, p. 38.

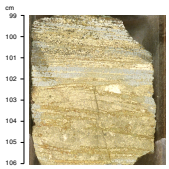

Geophysical logging reveals the same type of vertical variation in the feeder zone that was observed in core. From 100 to 145 mbsf, the apparent resistivity reaches extremely high values in response to intense sulfide veining. Resistivity tends to decrease with depth, as do density and acoustic velocity, and porosity reaches the minimum values measured in this hole. The Formation MicroScanner (FMS) images give a very good picture of the vein network and of its change in density with depth. The DCZ is well imaged, and logging indicates that this zone is ~13 m thick. In contrast to the overlying intervals, sulfide veining is essentially absent in the DCZ. Below 210 mbsf, the sediments are only slightly altered, and the logs record changes in structure and lithology of the underlying succession of interbedded mudstones, siltstones, and sandstones. FMS images show a high level of fracturing related to faulting in two intervals (221–239 and 250–270 mbsf) that also have low resistivity and high porosity. However, core recovery from these intervals was poor and rocks with structures indicative of significant faulting were not present in the recovered core. The high gamma-ray counts and low density indicate dominantly clayey sediment in these zones. The tops of these two intervals are marked by a contact surface dipping 50° to the west. Between these two intervals, the FMS maps a succession of fractures dipping the same direction at about 50°–70°. A sharp decrease in X-rays derived from K (measured by the shipboard multisensor track) in core recovered above 292 mbsf may reflect fault-controlled hydrothermal circulation and alteration of the overlying rocks.

Feeder zone mineralization is also well developed in Hole 1035F on the south flank of the massive sulfide but is only weakly developed in Hole 1035D to the east and is absent below the massive sulfide horizons in Holes 1035A and 1035G to the west. The greater extent of the sulfide feeder zone mineralization north-south is consistent with structural control of fluid flow by rift parallel faulting. The DCZ is developed in approximately the same stratigraphic interval in Hole 1035F as observed in Hole 856H (Fig. F7), but pyrrhotite and sphalerite are more abundant than in the center of the system.

Drilling on the east and west flanks of the deposit in Holes 1035D and 1035A, respectively, was terminated near the top of the DCZ horizon (~175 mbsf) because of destruction of the tungsten carbide drill bits used in these holes. Although the core recovery in this interval was low, the material retrieved from this depth is intensely silicified turbiditic mudstone weakly veined by pyrrhotite. Penetration of this silicified zone in Hole 1035G using the more robust tricone bits used to drill Holes 856H and 1035F showed that mineralization at this horizon on the flanks of the deposit is more weakly developed and consists mostly of pyrite and pyrrhotite veins and replacements in silicified mudstone. ISS grains from a sample from this zone have not unmixed and have a composition that is more Fe rich than isocubanite (Fe:Cu 2.4), similar to ISS included in sphalerite from massive sulfide near the top of the deposit that formed as rapidly quenched chimney fragments (R. Zierenberg, unpubl. data; Goodfellow et al., 1993).

The silicified horizon above the DCZ appears to represent an important hydrologic control on the high-temperature hydrothermal system that formed the massive sulfide. The transition from predominantly vertical crack-seal veins in the upper part of the feeder zone to subhorizontal mineralization controlled by sedimentary texture at the base of the feeder zone indicates that cyclic overpressure capable of fracturing the rock only occurred near the seafloor. During periods when the high-permeability pathways represented by the veins were sealed, fluid was forced to flow laterally into the more permeable sandy turbidite units. Conductive cooling of this ponded hydrothermal fluid facilitated silica deposition (Janecky and Seyfried, 1984), thus sealing the top of this interval. Conductive cooling also resulted in precipitation of ISS, which is the least soluble of the sulfide minerals that are present in this deposit. Development of high-grade, copper-rich replacement-style mineralization below the sulfide feeder zone was not anticipated prior to drilling. Permeable horizons below ancient massive sulfide deposits on land represent potential exploration targets that may not have been tested, as exploration drill holes are often terminated once the feeder zone mineralization has been penetrated.

Two lines of evidence suggest that the silicified horizon at the top of the DCZ also controls present-day fluid circulation in this part of Middle Valley. Pore fluid collected from the deepest section of Hole 1035A has distinctly lower Cl and Na and higher Li and K than pore fluids from overlying sediments (Fouquet, Zierenberg, Miller, et al., 1998). The composition of the low-salinity fluid closely matches the composition of hydrothermal fluid collected from the 264°C hydrothermal vent located 300 m south on the flank of the ODP Mound (Butterfield et al., 1994).

Hole 1035F, which penetrated through the silicified zone, was observed by a television camera lowered down the drill string to be vigorously venting hydrothermal fluid. It thus appears that the silicified zone represents an impermeable caprock that prevents fluids from the hydrothermal reservoir zone developed in the upper igneous crust (Davis and Fisher, 1994) from reaching the seafloor, except in areas where the seal has been penetrated by fracturing or, more recently, by drilling (Zierenberg et al., 1998).

Massive Sulfide Deposits at ODP Mound

A second massive sulfide mound located ~350 m south of the BHMS deposit was investigated in a single drill hole. Hole 1035H was drilled

on a relatively flat bench near the southern peak of ODP Mound (Fig. F3). Only one hydrothermal chimney was known to be actively venting in the Bent Hill area before Leg 169. The Lone Star vent is located ~54 m north and 36 m east of Hole 1035H at the north end of ODP Mound. The vent site consists of a single anhydrite chimney issuing fluid at 264°C. A second area of hydrothermal activity was briefly observed during the camera survey before drilling Hole 1035H and was later visited and sampled by submersible. This vent site, Shiner Bock vent, is ~30 m north of Hole 1035H and was also venting 264°C fluid from an anhydrite chimney.

Hole 1035H recovered 238 m of mineralized rock, which included three massive sulfide zones interbedded with feeder zones and weakly mineralized sediments (Fig. F7). Sulfide-veined and impregnated sediment underlies the massive to semimassive sulfide zones and grades into nonmineralized sediment. The massive sulfide consists of coarse-grained pyrite variably infilled and replaced by sphalerite (5%–40%), magnetite (up to 30%), clay minerals, minor chalcopyrite, and traces of galena. Massive sulfide from this mound contains significantly more sphalerite than material recovered from the BHMS deposit.

The uppermost core (0–8.8 mbsf) recovered clastic vuggy pyrite and sphalerite and hydrothermally altered claystone. Between 8.8 and 30 mbsf is a unit of massive sulfide consisting of angular, variably sized clasts composed of pyrite, marcasite, and sphalerite with minor chalcopyrite and isocubanite in a matrix of finer grained clastic sulfides. Magnetite and hematite are present in variable amounts. The major nonsulfide phases are dolomite and ankerite. Underlying this massive sulfide is a sulfide feeder zone where fine sandstone, siltstone, and silty claystone are impregnated and cut by thin veins of pyrrhotite, pyrite, sphalerite, chalcopyrite, and anhydrite (30–55.2 mbsf). The feeder zone grades into weakly mineralized fine sandstone and claystone (55.2–74.6 mbsf).

Below this is a second unit of massive sulfide composed of pyrite, pyrrhotite, and sphalerite (74.6–84.2 mbsf) followed by a second feeder zone where siltstone and fine sandstone are veined and impregnated with pyrrhotite and chalcopyrite (80–123 mbsf). Sedimentary rocks are locally brecciated and hydrothermally altered to chlorite.

A third interval of base metal-rich massive sulfide consisting of compact to vuggy black sphalerite (40%–70% of the sulfides) with pyrite, magnetite, and talc or clay infilling voids was intersected (123–142.3 mbsf). Copper sulfides are a minor component in this interval. At the base of this massive sulfide zone, a short interval of highly altered and mineralized rocks rich in amphibole and epidote was recovered. Deeper in the section is a relatively complex feeder zone (142.3–190.3 mbsf) where three thin zones of massive to semimassive sulfide (between 150 and 154 mbsf, 162 and 163 mbsf, and 180.7 and 182.3 mbsf) are within sulfide-veined sediment. Silty claystone, siltstone, and sandstone are impregnated with Cu-Fe sulfides and hydrothermally altered to chlorite. The semimassive to massive sulfide with altered sediment contains as much as 80% Cu-Fe sulfide. Replacement by sulfide and hydrothermal silica preserve planar laminae and cross-bedding that occurred in the original sediment. This rock appears to be very similar to the banded Cu-Fe sulfide found in the DCZ in Hole 856H. Between 190.3 and 219.1 mbsf the sediments are less intensely mineralized. Interbedded claystone, siltstone, and sandstone are partly silicified and altered to chlorite and contain veinlets and impregnation of Cu-Fe sulfides. The last section was cored in hemipelagic and turbiditic sediment

(219.1–247.9 mbsf) that is partly silicified, weakly chloritized, and contains anhydrite molds. Minor disseminated pyrite is present locally in this interval.

Multiple episodes of hydrothermal discharge are clearly evident in the section drilled below the ODP Mound. The presence of three stacked sequences of massive sulfide underlain by feeder zone mineralization encountered over a depth interval of 210 m is an indication of episodic hydrothermal discharge. Lower sulfide horizons are locally very coarse grained and have been extensively recrystallized in response to the passage of hydrothermal fluids that formed overlying massive sulfide zones. Estimation of mineral abundance, supplemented by limited onboard geochemical analyses, shows that the material recovered from this hole is a much higher grade (2.9%–51% Zn, 0.12%–0.62% Cu) than massive sulfide from the Bent Hill deposit. High-grade (8.0%–16.6% Cu), Cu replacement mineralization is present in approximately the same stratigraphic horizon as encountered below the BHMS and raises the question of the possible continuity of the DCZ mineralization between the two deposits (Fouquet, Zierenberg, Miller, et al., 1998).

Drilling at this site also reinitiated hydrothermal venting, similar to that at Hole 1035F. The intensity of the hydrothermal flow out of the 25-cm-diameter borehole was sufficient to carry drill cuttings of sedimentary rock 3 cm in diameter, and massive sulfide fragments up to 0.5 cm in diameter, more than 10 m above the seafloor. This violent venting suggests that the drilling penetrated into an overpressured zone (Zierenberg et al., 1998). The Ridge Inter-Disciplinary Global Experiments (RIDGE) program of the U.S. National Science Foundation initiated an event-response cruise using the *Thomas G. Thompson* in an effort to sample the vent fluids to establish a baseline for recognizing compositional changes in the vents and to evaluate the microbiological response to initiation of hydrothermal venting. By the time the site was visited with the Canadian remotely operated vehicle *ROPOS* 3 weeks later, the velocity of venting had slowed considerably and 272°C hydrothermal fluid was venting from a 1-m-high anhydrite-rich chimney that had grown in the bore hole opening (D.S. Kelley and M.D. Lilley, unpubl. data). This chimney had grown to a height of ~9 m when visited by the *Alvin* submersible in 1998 (R. Zierenberg, unpubl. data).

Active Hydrothermal Circulation in the Dead Dog Area

The Dead Dog vent field is the primary locus of hydrothermal venting in Middle Valley with at least 20 active high-temperature (250° to 276°C; Ames et al., 1993) hydrothermal vents. Investigations during Leg 169 included drilling near an active hydrothermal mound (Site 1036), deployment of pop-up pore pressure instruments (PUPPIs), and reinstrumentation of seal bore holes at Sites 858 and 857.

Site 1036 targeted the active Dead Dog Mound (Fig. **F4**) in order to (1) constrain the fluid flow rates and pathways for hydrothermal fluid and seawater entrained into the hydrothermal upflow zone, (2) study the mode of formation of the hydrothermal mounds, (3) determine the effects of hydrothermal activity on sediment diagenesis and alteration, and (4) determine the presence, continuity, and nature of a suspected caprock horizon at ~30 mbsf. In order to meet these objectives, we drilled Holes 1035A, 1035B, and 1035C along a northwest-southeast transect from the top to the margin of the 7-m-high Dead Dog active hydrothermal mound. Hole 1036A was located ~9 m west of a 268°C hydrothermal vent and was cored to 38.5 mbsf. Hole 1036B was offset

~37 m to the northwest and cored to a depth of 52.3 mbsf through the edge of the mound. Hole 1036C was offset another 34 m to the northwest and cored to a depth of 54.2 mbsf in an area within the vent field, but between hydrothermal mounds.

The results from the drilling at Site 1036 showed that Holocene- to late Pleistocene-age hemipelagic sequence of flat-lying silty clay has a relatively consistent thickness between holes (25.09 m at Hole 1036A, 25.60 m at Hole 1036B, and 26.70 m at Hole 1036C). The ~7-m-high relief of the Dead Dog Mound is close to the stratigraphic thickness of a unit of chimney-derived rubble that was recovered in Hole 1036A drilled on top of the mound. This unit is a heterogeneous mixture of clasts derived from the collapse of anhydrite chimneys, now partly altered to gypsum, greenish gray clay (probably a Mg-bearing smectite), and fine-grained pyrrhotite with subordinate pyrite and sphalerite. The lowermost 1.6 m of the sequence has a dark color, probably a result of the slow, ongoing process of gypsum dissolution, leaving behind a residue of clay and sulfide. Silty clay of apparent hemipelagic origin was recovered from beneath the chimney debris at Hole 1036A but is present at the surface of the seafloor at Holes 1036B and 1036C. The mound appears to be entirely a buildup of rubble and did not form by inflationary growth through precipitation of authigenic hydrothermal minerals in the subsurface, nor are the mounds formed by tectonic uplift. The Dead Dog Mound is presumably a recently formed feature built upon the Holocene fill of Middle Valley.

Hydrothermal alteration boundaries are zoned away from the upflow conduit that feeds the Dead Dog vent (Goodfellow and Peter, 1994.). The boundaries of an upper authigenic carbonate alteration zone and a lower anhydrite alteration zone deepen away from the mound, reflecting the decreasing geothermal gradients. The core from Hole 1036A contains just a few dolomite nodules in the sediment underlying the chimney-derived rubble. In the core from Hole 1036B, numerous dolomite and calcite nodules are found in the interval from 10.20 to 32.20 mbsf. Hydrothermal alteration also affected the preservation of microfossils in the cores. Core-catcher samples prepared for paleontological analysis were devoid of foraminifers below 9.5 mbsf in Hole 1036A, below 18.6 mbsf in Hole 1036B, and below 35.0 mbsf in Hole 1036C. Siliceous microfossils disappear at even shallower burial depths in all the holes. The depth at which the magnetic susceptibility of sediments decreases to near zero because of hydrothermal alteration (magnetic wipeout zone) also increases with distance from the vent.

Authigenic anhydrite is present as disseminated crystals, nodules, and cement and is a distinctive alteration facies of the hydrothermal system. The depth of first appearance of anhydrite was 9.5 mbsf in Hole 1036A, 18.55 mbsf in Hole 1036B, and 42.20 mbsf in Hole 1036C. Anhydrite forms by the mixing of Ca-rich, sulfate-depleted hydrothermal fluids with sulfate-bearing seawater that is drawn into the upper portions of the hydrothermal vent field in response to rapid fluid upflow (Glenn, 1998; Stein and Fisher, in press). Normal seawater concentrations are present in pore fluids sampled from shallow depths, but indicate seawater recharge and high-temperature sediment alteration at depth (Fouquet, Zierenberg, Miller, et al., 1998). PUPPIs deployed in the area of the drilling transect also recorded differential pore pressure indicative of localized seawater recharge (Schultheiss, 1997). Anhydrite has inverse solubility and becomes less soluble at higher temperatures. Experimental data (Bischoff and Seyfried, 1978) and geochemical modeling (Janecky and Seyfried, 1984) indicate the depth to the top of the

anhydrite precipitation zone represents the approximate position of the 160°C isotherm. Fluids with compositions similar to those sampled at Dead Dog vent are present below 40 mbsf in the cores from Hole 1035B. Inflow of cold seawater may also have influenced the abundance and distribution of subseafloor microbes by preventing the flux of H_2S though near-surface sediments where in situ temperatures below the upper thermal limits for hyperthermophiles occur (Cragg et al., **Chap 2,** this volume; Summit et al., **Chap. 3,** this volume).

Although Hole 1036A is only 9 m away from an active vent, no major hydrothermal vein network was intercepted at depth and the uppermost sediments are not highly lithified by hydrothermal alteration. Only a few hydraulic breccias and some anhydrite veins were recovered. The absence of a stockwork zone underlying the mound and the lack of extensive induration suggest that the Dead Dog hydrothermal mound is an immature feature, consistent with the occurrence of collapsed chimney material overlying very young sediments. Hydrothermal lithification (silicification?) increases with depth to the point that in each of the holes, the XCB cutting shoe was destroyed in cutting the lowermost core at ~50 mbsf.

An important scientific objective for Leg 169 was to replace the existing CORK and thermistor strings installed in Holes 857D and 858G as part of an active hydrologic flow experiment designed to enable temporal monitoring of changes in subseafloor temperature and pore pressure. The operation plan at Hole 857D was to replace the 300-m-long thermistor string installed during Leg 139, which was entirely within the cased section of the hole, with an 898-m-long thermistor string that would provide temperature information extending across the area of the hole with high hydraulic conductivity extending to near the bottom of the hole (Fig. **F11**). An attempt to replace this thermistor string during Leg 146 had damaged the existing CORK. The borehole seal of the CORK in Hole 858G had also failed and was observed on *Alvin* dives in 1993 to be venting hydrothermal fluid. An array of ocean bottom seismometers (OBS) had been deployed by scientists at Scripps Institution of Oceanography in advance of the drilling in an attempt to monitor fracturing that could be induced by allowing cold seawater to flow into the hot formations. If the holes were sealed and had recovered to thermal equilibrium with the surrounding sediment, then opening the holes to overlying cold seawater could result in a significant overpressure relative to the hot hydrostatic head. A hole-to-hole hydrologic experiment was planned to monitor the pressure in Hole 858G generated in response to a transient pressure pulse to be induced by removing the CORK from Hole 857D, which is located 1.6 km to the south.

Initial observation of the CORK in Hole 858G from the vibration-isolated television camera revealed no evidence that the fluid flow observed earlier was continuing. Upon recovery of the lower half of the CORK housing, we discovered that the inside housing of the CORK body was coated with hydrothermal precipitates, predominantly anhydrite, but with abundant pyrrhotite and pyrite. Naturally occurring hydrothermal chimneys from the Dead Dog vent field are predominantly composed of anhydrite, with only minor amounts of pyrite and trace amounts of pyrrhotite. A water sampling temperature probe (WSTP) run 20 m into the casing indicated fluid temperatures >220°C prior to failure of an O-ring in the tool. The fluid sample collected contained a mixture of seawater and hydrothermal fluid that extrapolates to a hydrothermal end-member similar to fluids sampled by *Alvin* in the vent field. A temperature run with the Geothermal Resources Council ultra-

F11. Middle Valley holes reinstrumented with CORKs, p. 39.

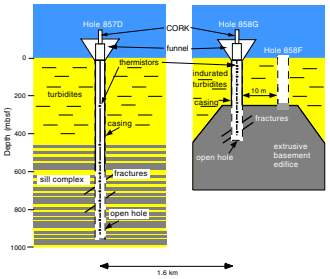

high-temperature multisensor memory dewared tool indicated that the borehole was essentially isothermal at 272°C (near the maximum measured in the vent field) at depths below 85 mbsf. The temperature tool could only be run to 205 mbsf because of an obstruction in the cased portion of the drill hole. A wash core was recovered from an unlined core barrel and is believed to be representative of the material drilled from inside the casing at depths below the blockage at 205 mbsf. The wash core was predominantly loosely aggregated, fine-grained pyrrhotite and pyrite with minor amounts of anhydrite. Fluid sampled from the wash core had a very low magnesium content consistent with a high temperature origin and minimal dilution with seawater. The composition of this fluid sample is very similar to vent fluids collected in the Dead Dog field.

It was anticipated that removal of the CORK from Hole 857D would result in a rapid inflow of water into the hole as observed during Leg 139 by packer and flowmeter experiments. Temperature profiles and fluid samples confirmed that cold seawater was entering the hole. The new thermistor string was installed, and the hole was resealed with a new CORK. Subsequent measurements downloaded from the CORK data loggers provide the first detailed characterization of the downhole temperature profile in a seafloor hydrothermal field (Davis and Becker, 1998) and determined the pressure gradient that drives fluid from the vicinity of Hole 857D toward Hole 858G in the Dead Dog vent field.

Escanaba Trough

General Comparison to Middle Valley Deposits

Escanaba Trough provides an interesting contrast to Middle Valley. The two sites share many similarities; both are sediment-buried spreading centers covered by ~500 m of Pleistocene turbiditic sediments, and each site hosts older large massive sulfide deposits as well as active hydrothermal vent sites that are not presently depositing massive sulfide. Differences between the sites include a lower spreading rate at Escanaba (2.4 vs. 5.8 cm/yr) and lower background heat flow such that the projected temperatures at the sediment/basalt interface are ~80°C for Escanaba vs. ~270°C for Middle Valley (Davis and Becker, 1994a; Davis and Villinger, 1992). There are pronounced differences in the composition of the hydrothermal deposits as well. Trace element and lead isotope compositions of massive sulfide from Escanaba Trough require a significantly higher contribution of sedimentary-derived components (Zierenberg et al., 1993; Koski et al., 1994). The active hydrothermal vents at Escanaba Trough are lower temperature (220° vs. 285°C) and also have a higher concentration of components derived by hydrothermal leaching from sedimentary sources (Campbell et al., 1994). A primary objective of the drilling was to attempt to understand the reasons for the compositional differences between the Middle Valley and Escanaba Trough hydrothermal systems.

Escanaba Trough Reference Site

Site 1037 was drilled near the spreading axis ~5 km south of the known area of hydrothermal venting to provide a reference section through relatively unaltered sedimentary fill of Escanaba Trough. This site provided an important insight into the rapid infilling of Escanaba Trough by large scale turbidites. Recovery from Hole 1037B included a

relatively complete sedimentary sequence of the Escanaba Trough fill sediment between 0 and 495.6 mbsf (Fouquet, Zierenberg, Miller, et al., 1998). Metamorphosed claystone and siltstone was recovered beneath this sequence between 495.6 and 507.8 mbsf. Basaltic rocks were recovered from 507.8 mbsf to the base of the hole at 546 mbsf.

Sedimentology and Sediment Geochemistry

Zuffa et al. (2000) defined six major lithostratigraphic units on the basis of sand/silt-dominant vs. mud-dominant turbidites and changes in composition and sedimentary structure and magnetic susceptibility data that assisted in distinguishing graded turbidites in fine-grained units.

Unit A (0–1.7 mbsf) consists of Holocene hemipelagic fossiliferous greenish gray clay. A ^{14}C date on planktonic foraminifers indicates a sedimentation rate of 0.17 cm/yr (Brunner et al., 1999), which is consistent with previous determinations of the Holocene sedimentation rate from Escanaba Trough (Karlin and Lyle, 1986).

Unit B (1.7–120.6 mbsf) is the uppermost of a series of fining- and thinning-upward sequences that record extremely rapid burial of Escanaba Trough by megaturbidite beds. In the lowermost 50 m of this unit, only massive fine- to medium-grained sand was recovered. Coring disturbance in this unit precludes definitive determination of the sedimentary history, but Zuffa et al. (2000) interpret this sand interval as the base of a single megaturbidite flow (120.6–63.5 mbsf) that grades upward to pelite. This thick sand-rich interval is at the depth from which petrographically similar sands were recovered from Deep Sea Drilling Project Hole 35, drilled ~15 km to the south. Davis and Becker (1994b) correlated this massive sand interval with an acoustically transparent horizon mapped by single-channel seismic reflection profiling and speculated that it was deposited as the result of the floods draining glacial Lake Missoula. The overlying interval (63.5–1.7 mbsf) contains 10 thinning-upward megaturbidite beds.

Unit C (120.6–177.6 mbsf) is a fining- and thinning-upward sequence similar to Unit B including a 35-m-thick, poorly sorted, fine- to medium-grained sand at the base that Zuffa et al. (2000) interpret as three megaturbidite beds.

Unit D (177.6–366.6 mbsf) is a finer grained unit dominated by mud-rich turbidites. The individual turbidites can exceed 10 m in thickness but generally have only thin basal units of silt or very fine-grained sand.

Unit E (366.6–495.6 mbsf) consists predominantly of turbiditic beds with siltstone bases. Individual depositional units in this interval are thinner than in overlying units. Sedimentary structures typical of turbidites (parallel, wavy, and cross laminations) are more common than in the overlying megaturbidite sequence.

Core recovery was poor between 495.6 and 507.8 mbsf, but most of the cored material is silicified calcareous claystone rubble. These rocks are just above the transition from Escanaba Trough sediment fill to igneous basement and have been thermally altered. Metamorphic minerals include euhedral quartz, zoned plagioclase feldspar, brown biotite, and in the deepest samples, epidote and actinolite (Fouquet, Zierenberg, Miller, et al., 1998).

Brunner et al. (1999) determined sedimentation rates for Hole 1037B based on foraminiferal assemblages and accelerator mass spectrometer ^{14}C dating of planktonic foraminifers. Average depositional rates be-

tween 11 ka and 32 ka were >10 m/k.y., an amazingly fast rate for sediments deposited at 3200 mbsl. The ages of the upper 120 m of turbidites coincide with the formation of the channeled scabland deposits formed by catastrophic draining of glacial Lake Missoula. Brunner et al. (1999) interpret the uppermost turbiditic fill of Escanaba to be derived from hyperpycnal turbidite flows generated as jökulhlaups from glacial Lake Missoula entered the ocean near the present mouth of the Columbia River. Previous work by Vallier et al. (1973) had identified the Columbia River Basin as the source of the pyroxene-bearing sands cored in Escanaba Trough. Sedimentary petrography on samples collected during Leg 169 confirms the Columbia River basin as the dominant sedimentary source for most of the Escanaba Trough sediment fill. Zuffa et al. (2000) suggest that the compositional changes in heavy mineral assembles downcore that were previously interpreted to reflect a change with depth to a source area dominated by material derived from the Klamath mountains is instead related to selective dissolution of pyroxene downcore. Based on detailed near-surface seismic reflection profiles, bathymetric data, and sidescan sonar data, Zuffa et al. (2000) determined that turbidites have reached Escanaba Trough by flow down the Cascadia Channel, along the Blanco Fracture Zone, south across the Tufts Abyssal Plain to the Mendocino Escarpment, and eventually northward into Escanaba Trough (Fig. **F5**), a journey of >1100 km. The thickest sedimentary beds are interpreted to represent frozen turbidites that entered the box canyon defined by Escanaba Trough where they stopped, dropping their entire sedimentary load.

The rapid sedimentation rate in the Escanaba Trough helps to preserve the chemical signatures in pore waters, and pore-water concentration-depth profiles are likely to correlate with in situ diagenetic changes little modified by diffusion. Concentration profiles of several species (Li, Na, and Cl) show local maximum at 360 mbsf. Li and Na also increase as basement is approached, as do Ca, Sr, B, and Cl (James and Palmer, 1999; Gieskes et al., **Chap. 1,** this volume). Most of the dissolved elements have lower concentrations as basement is approached. In contrast, K and Mg generally have values decreasing below seawater concentrations with depth, but concentrations increase again just above the igneous rocks. Sulfate is depleted within the upper 100 m of the sediment column by bacterial sulfate reduction. Diagenetic reaction in these sediments apparently provides a net source of B, Li, Na, Ca, Sr, and NH_4 to pore waters. A decrease in Mg and K concentration with depth is interpreted as being caused by clay-mineral formation.

The organic matter in the sediments of this reference site is generally immature from the top to ~450 mbsf. There are a few horizons with more mature bitumen, which is interpreted to be derived from recycled, older sedimentary detritus carried in by turbidites; however, the low extract yields throughout the hole indicate that there are no petroleum zones. Below 450 mbsf, the organic matter is thermally altered, but low concentrations of bitumen reflect in situ maturation without migration/expulsion, suggesting that the thermal event that resulted in metamorphism of the lowermost sediments was not accompanied by extensive fluid circulation higher in the sediment column. Temperatures recorded during coring of the uppermost sediments show a generally linear increase to 15°C at 85 mbsf, the deepest measurement. Extrapolation of the thermal gradient indicates a temperature of 84°C at 500 mbsf, the approximate depth of the sediment basalt interface (Fouquet, Zierenberg, Miller, et al., 1998). These data are consistent with surface heat-flow measurements (Davis and Becker, 1994b) and in-

dicate that the thermal pulse responsible for organic maturation and sediment alteration has decayed.

The nature of the transition from sediments into the uppermost igneous crust differs from the thick-sheeted sill complex encountered in Middle Valley. Chilled margins and an absence of any recovered sedimentary interbeds suggests that the uppermost basalts are flows. The basaltic rocks recovered from ~530 mbsf to the base of the hole (546 mbsf) range from fine- to coarse-grained and appear to be a single cooling unit, most likely a thick, ponded flow. Although the basalts are generally fresh appearing, there are indications of postcrystallization thermal alteration, consistent with the evidence for metamorphism of the overlying sediments. Alteration minerals are generally vein controlled and include smectite, chlorite, albite, and actinolite/Mg hornblende. Veins completely filled with interpenetrating, fine acicular Mg hornblende crystals up to 2 mm long are locally abundant, indicating the presence of relatively high temperature (~350°C?) hydrothermal fluids. However, the lack of pervasive hydrothermal alteration of the basalt is consistent with a local, short-lived thermal event, perhaps driven by a shallow subvolcanic sill (Fouquet, Zierenberg, Miller, et al., 1998).

Central Hill Area

A transect of holes (Holes 1038A to 1038I) was drilled across Central Hill in Escanaba Trough with the highest priority being to drill through the massive sulfide deposits and into the alteration zone near the center of the hydrothermal upflow zone (Fig. F6). A primary objective was to establish the causes of the major compositional differences between the deposits at Middle Valley and Escanaba Trough. A series of shallow RCB exploratory holes was targeted primarily at the exposed mounds of massive sulfide in order to establish the extent, composition, and drilling potential and conditions of the massive sulfide in this area prior to starting a deeper drill hole. Drilling conditions, especially in the massive sulfides, proved difficult and our understanding of this site is hampered by generally low core recovery. Regardless, the drilling at Site 1038 provided important information that allows us to interpret the differences between the Middle Valley hydrothermal system and that at Escanaba Trough.

Massive sulfide recovered from Central Hill suggests that the mineralization forms only a thin (5–15 m) veneer over the sediment. No major intersection of massive sulfides was recovered. In each hole started on massive sulfide outcrops, the inferred thickness of the massive sulfides was similar to the extent of sulfide mound build-up above the seafloor as observed on submersible dives. Seafloor observations had indicated that this system was much younger than the massive sulfides at Bent Hill (Zierenberg et al., 1993), and drilling did not encounter any sediment-buried sulfide deposits. The sulfide samples recovered were dominantly massive pyrrhotite with abundant pyrite in some samples. Much of the pyrite formed by replacement of earlier pyrrhotite. Several samples contain abundant sphalerite, and minor amounts of Cu-Fe sulfide are present in some samples. Gangue minerals are minor with barite as the predominant phase (Fouquet, Zierenberg, Miller, et al., 1998).

A characteristic difference between this site and the Bent Hill deposit in Middle Valley is the absence of a well-developed vein-dominated feeder zone in the sediment under the sulfide mounds. Chlorite is the dominant alteration mineral in samples recovered beneath the massive

sulfide deposits (Lackschewitz et al., **Chap. 6,** this volume). Changes in the properties of magnetic minerals from samples collected below massive sulfide mounds also indicate hydrothermal alteration (Urbat et al., 2000). The well-developed hydrothermal lithification, silicification, and sulfide veining that characterizes the feeder zone mineralization beneath the Bent Hill deposit was not encountered at Escanaba Trough. The extensive surface exposure of relatively small massive sulfide mounds coupled with the lack of development of a distinct feeder zone suggests that hydrothermal venting was probably diffuse and short lived. This is consistent with the lack of chimneys, an indication of focused fluid discharge, and the occurrence of thin, high-temperature pyrrhotite crusts on the sediment observed during submersible dives (Zierenberg et al., 1993).

Sedimentology

Incomplete core recovery precludes detailed correlation of sedimentary units between Sites 1037 and 1038. Using grain-size and magnetic susceptibility data, a correlation can be made between the upper 100 m of cores from Holes 1038A, 1038B, 1038G, 1038I, and the reference hole (Hole 1037B). Biostratigraphic correlation is precluded because most samples examined from Site 1038 contain very few foraminifers or are barren. Alteration of foraminifers is clearly associated with thermal and hydrothermal effects. However, Hole 1038F provides confirmation that Holocene sedimentation is exceptionally fast, probably >290 cm/k.y.

Stratigraphic correlation is more tenuous below 100 mbsf. Hole 1038I was drilled near the flat-topped apex of Central Hill and is the only hole that penetrated through the sediment fill to igneous rocks presumed to represent the uppermost oceanic crust. The most reasonable interpretation of the sedimentary sequences suggests that each of the lithostratigraphic units defined on board the *JOIDES Resolution* for Hole 1037B can be correlated with Hole 1038I within the depth of a single coring interval (~10 m). This interpretation implies that the lowermost 100 m of sediment section deposited above the basaltic rocks in Hole 1037B are not present above the basaltic rocks drilled at the base of Hole 1038I. The depth to the seafloor at Hole 1036I is 85 m shallower than at Hole 1037B and the apex of Central Hill has been uplifted ~110 m above the surrounding turbidite fill. Data from detailed seismic profiling (Davis and Becker, 1994b; Zuffa et al., 2000), sediment coring (Normark et al., 1994; Karlin and Zierenberg, 1994), submersible observations (Zierenberg et al., 1994), and sidescan sonar (Ross et al., 1996) indicate that the uplift of Central Hill occurred during the Holocene and postdates the deposition of the valley-filling turbidites.

Near-surface (upper 3 m) sands lack lateral continuity across Central Hill, suggesting that they may have been locally derived, perhaps by slumping off the steep fault scarps that surround the basin. Sediment debris flows recovered by gravity coring indicate that slumping of sediment accompanied uplift of Central Hill (Normark et al., 1994). Submersible observations near the crest of Central Hill revealed steep scarps and erosional channels interpreted to have formed by local mass flow (Zierenberg et al., 1994). The thick sand horizon that characterizes the base of Unit B in Hole 1037B can be correlated with sands recovered at Site 1038. The top of this interval is identified in all holes that penetrated to a depth >80 mbsf. This unit is interpreted to be correlative to the top of the regionally developed transparent seismic layer (Davis and

Becker, 1994b). Despite the fact that there is 40 m of relief between Holes 1038B and 1038I, the top of this sand is present within 6.1 m of the same depth in all the holes, which implies that the topographic expression of Central Hill is predominantly caused by slumping along normal faults and that significant sections of the sedimentary cover have not been removed.

Igneous Petrology

A basaltic layer from 1 to at least 5 m thick was intersected in three holes (Holes 1038G, 1038H, and 1038I) at depths between 142 and 162 mbsf. Adjusted for elevation of the top of the hole, this unit is at a near-constant elevation of 3365–3385 m and appears to slope from west to east. A flat-lying seismic reflector interpreted as either a basaltic flow or sill was mapped at the same depth to the east of Central Hill across the innermost rift bounding fault (Zierenberg et al., 1994). This unit could be either a thin flow erupted on sediment or a thin sill intruded near the top of the sand-rich horizon that defines the top of Unit C in Hole 1037B. Recovered fragments of basalt contained quenched margins, but contact relationships with the sediment were disturbed by drilling.

Basalt was also intersected at the base of Hole 1038I (403 mbsf). A contact was recovered that had 2 mm of baked and bleached sediment underlain by 5 mm of fresh glass. Time constraints at the end of the leg permitted only 1.5 m of penetration into the basalt, and all of the recovered core appeared to be from one cooling unit. The depth to this basalt coincides with a seismic reflector that is directly under Central Hill and sits ~100 m above the poorly defined sediment basalt contact in the Central Hill area (Zierenberg et al., 1994). The evidence at hand is consistent with this unit being a basaltic sill intruded near the base of the sediment section. Intrusion of this sill may have been responsible for the localized uplift of Central Hill, in accordance with the models presented by Davis and Becker (1994b), Denlinger and Holmes (1994), and Zierenberg et al. (1994) to account for the topography and hydrothermal history of Escanaba Trough.

Geochemistry

Pore fluids collected from Site 1038 show a wide range in chemical compositions and provide important insight into the history of the hydrothermal system that formed the massive sulfide deposits. Comparison of pore fluids with hydrothermal fluids sampled from the active vents in 1988 (Campbell et al., 1994) shows that a hydrothermal component is obvious in all the holes and dominates pore-fluid chemistry at shallow depths below hydrothermally active and inactive sulfide mounds. One of the most surprising results of drilling at Site 1038 was the discovery that pore fluid Cl concentration ranges from 300 to 800 mM, indicating the presence of hydrothermal fluid affected by phase separation. The relationship between the Na and Ca content with Cl fits on a mixing line, indicating a single source for the high- and low-Cl fluids. Because most of the holes are relatively shallow, the high-salinity component dominates pore fluids. Low-salinity pore fluid is particularly evident in sand-rich layers between 80 and 120 mbsf in Holes 1038A, 1038H, and 1038I and is dominant below 190 mbsf in Hole 1038I.

The thermal gradient in the upper part of Hole 1038I is ~2°C/m, but the deepest measurement was at 56.8 mbsf, where a temperature of

115.9°C was measured. The highest vent temperature measured at this site was 220°C (Campbell et al., 1994). Rapid lateral advection of 220°C hydrothermal fluid through the massive sand layer at a depth of ~110 mbsf could conceivably support a 2°C/m thermal gradient and could supply the active hydrothermal vents. However, the hydrothermal vents have salinities above that of seawater, as do pore fluids sampled beneath massive sulfide, whereas the sandy horizon seems to contain low-salinity pore fluids. High-salinity pore fluid is also present immediately below the basaltic sill(?) in Holes 1038H and 1038I (Gieskes et al., **Chap. 1,** this volume). If the 2°C/m linear temperature gradient measure in the shallow portion of Hole 1038I continued to depth, temperatures at depths greater than ~200 mbsf would be in the range needed for phase separation. Although we were not able to measure temperatures below 57 mbsf in Hole 1038I, it would appear very unlikely that the high thermal gradient continues much deeper. The deepest sediments recovered from Hole 1038I showed less evidence for enhanced lithification and thermal alteration than rocks collected at in situ temperatures of 270°C in Middle Valley. Evidence for high downhole temperatures for holes drilled in Middle Valley, such as melting of core liners or seals, were not encountered at Escanaba Trough.

Even if the present thermal regime is not hot enough to promote phase separation of seawater-derived hydrothermal fluids, the presence of both high- and low-salinity components in the pore waters is an indication that the temperature pulse that caused a phase separation must have been recent relative to the time scale of diffusion of fluids through sediment (a few tens of years?). High temperatures are also indicated by the low concentration of Mg below 100 mbsf and by concentrations of Li and B below 300 mbsf that are far higher than those recorded in the reference hole (James and Palmer, 1999).

The organic geochemical data collected on board ship also support the notion of an intense, but brief, heating of the sediments. High concentrations of thermogenic methane were found in Holes 1038E, 1038H, 1038F, 1038G, and at depths greater than 40 mbsf in Hole 1038I. The presence of benzene and toluene confirm high-temperature cracking of organic matter. Bitumen fluorescence indicates a high maturation temperature of 150° to 250°C. The estimated temperature of organic maturation is higher than in Middle Valley. The regional maturation of organic matter has been rapid for all holes. In Hole 1038I, organic matter maturation occurred in situ without migration and is complete at a depth of ~160 mbsf, indicating high heat flow, but only limited flow of hydrothermal fluid through the sediment (Fouquet, Zierenberg, Miller, et al., 1998).

SUMMARY

The comparisons between Middle Valley and Escanaba Trough suggest the following generalities. Creation of new oceanic crust by seafloor spreading and burial of oceanic crust by sedimentation occurred at approximately the same rate in Middle Valley, such that the uppermost oceanic crust is a transitional zone of sheeted sills. Slower spreading at Escanaba, along with exceptionally rapid sedimentation rates, suggests that much of Escanaba basement formed by seafloor eruption of basalt that was later buried by sediment. Periodic large-scale eruptions led to the emplacement of large intrusions near the sediment/basalt interface, such as the one postulated to have uplifted Central

Hill, and occasionally to the emplacement of basalt flows over the sediment fill, as observed to the east of Central Hill.

The Central Hill area has experienced a recent high-temperature event that flushed the sediment column with high temperature hydrothermal fluids. Evidence of the passage of these fluids through the sediment is the extensive alteration of the organic matter in the sediment and local alteration of sediment to chlorite. Massive sulfide deposits formed from these fluids are extensive, but the mineralization is predominately located at the sediment/water interface and feeder zone–style mineralization is rare. The sulfides are dominated by high-temperature hexagonal pyrrhotite, but the sulfides are enriched in elements such as Pb, As, Sb, and Sn that are derived from the sediments.

In contrast, the hydrothermal system responsible for the development of massive sulfide deposits in Middle Valley seems to have been long lived and highly focused allowing the formation of massive sulfide >100 m thick. The Bent Hill deposit is underlain by an extensive hydrothermal feeder zone. A silicified horizon below the base of the feeder zone provided a hydrologic seal on the system that alternately allowed focused fluid upflow where breached by fault zones and resulted in extensive subseafloor hydrothermal replacement mineralization when fluids were prevented from venting to the seafloor. Repeated development of hydrothermal systems at ODP Mound are indicated by stratigraphically stacked massive sulfide lenses, each underlain by associated feeder zone mineralization. This suggests that deeper structures, such as ridge-parallel normal faults or the transition from sediment-rift type to normal oceanic crust controlled the location of hydrothermal discharge.

REFERENCES

Ames, D.E., Franklin, J.M., and Hannington, M.H., 1993. Mineralogy and geochemistry of active and inactive chimneys and massive sulfide, Middle Valley, northern Juan de Fuca Ridge: an evolving hydrothermal system. *Can. Mineral.,* 31:997–1024.

Bischoff, J.L., and Seyfried, W.E., 1978. Hydrothermal chemistry of seawater from 25°C to 350°C. *Am. J. Sci.,* 278:838–860.

Bjerkgård, T., Cousens, B.L., and Franklin, J.F., in press. Metal sources for the Middle Valley sulfide deposits, Northern Juan de Fuca Ridge. *Econ. Geol.*

Brunner, C.A., Normark, W.R., Zuffa, G.G., and Serra, F., 1999. Deep-sea sedimentary record of the late Wisconsin cataclysmic floods from the Columbia River. *Geology,* 27:463–466.

Butterfield, D.A., McDuff, R.E., Franklin, J., and Wheat, C.G., 1994. Geochemistry of hydrothermal vent fluids from Middle Valley, Juan de Fuca Ridge. *In* Mottl, M.J., Davis, E.E., Fisher, A.T., and Slack, J.F. (Eds.), *Proc. ODP, Sci. Results,* 139: College Station, TX (Ocean Drilling Program), 395–410.

Campbell, A.C., German, C.R., Palmer, M.R., Gamo, T., and Edmond, J.M., 1994. Chemistry of hydrothermal fluids from the Escanaba Trough, Gorda Ridge. *In* Morton, J.L., Zierenberg, R.A., Reiss, C.A. (Eds.), *Geologic, Hydrothermal, and Biologic Studies at Escanaba Trough, Gorda Ridge, Offshore Northern California*. U.S. Geol. Surv. Bull., 2022:201–221.

Currie, R.G., and Davis, E.E., 1994. Low crustal magnetization of the Middle Valley sedimented rift inferred from sea-surface magnetic anomalies. *In* Mottl, M.J., Davis, E.E., Fisher, A.T., and Slack, J.F. (Eds.), *Proc. ODP, Sci. Results,* 139: College Station, TX (Ocean Drilling Program), 19–27.

Davis, E.E., and Becker, K., 1998. Borehole observatories record driving forces for hydrothermal circulation in young oceanic crust. *Eos,* 79:369.

————, 1994a. Formation temperatures and pressures in a sedimented rift hydrothermal system: ten months of CORK observations, Holes 857D and 858G. *In* Mottl, M.J., Davis, E.E., Fisher, A.T., and Slack, J.F. (Eds.), *Proc. ODP, Sci. Results,* 139: College Station, TX (Ocean Drilling Program), 649–666.

————, 1994b. Thermal and tectonic structure of the Escanaba Trough: new heatflow measurements and seismic-reflection profiles. *In* Morton, J., Zierenberg, R.A., and Reiss, C.A. (Eds.), *Geologic, Hydrothermal, and Biologic Studies at Escanaba Trough, Gorda Ridge, Offshore Northern California*. U.S. Geol. Surv. Bull., 2022:45–64.

Davis, E.E., Currie, R.G., and Sawyer, B.S., 1987. Marine geophysical maps of western Canada: regional SeaMARC II acoustic image mosaics and Sea Beam bathymetry. *Geol. Surv. Can.,* Maps 2-1987 through 17-1987 (scale 1:250,000).

Davis, E.E., and Fisher, A.T., 1994. On the nature and consequences of hydrothermal circulation in the Middle Valley sedimented rift: inferences from geophysical and geochemical observations, Leg 139. *In* Mottl, M.J., Davis, E.E., Fisher, A.T., and Slack, J.F. (Eds.), *Proc. ODP, Sci. Results,* 139: College Station, TX (Ocean Drilling Program), 695–717.

Davis, E.E., Mottl, M.J., Fisher, A.T., et al., 1992. *Proc. ODP, Init. Repts.,* 139: College Station, TX (Ocean Drilling Program).

Davis, E.E., and Villinger, H., 1992. Tectonic and thermal structure of the Middle Valley sedimented rift, northern Juan de Fuca Ridge. *In* Davis, E.E., Mottl, M.J., Fisher, A.T., et al., *Proc. ODP, Init. Repts.,* 139: College Station, TX (Ocean Drilling Program), 9–41.

Denlinger, P., and Holmes, M.L., 1994. A thermal and mechanical model for sediment hills and associated sulfide deposits along Escanaba Trough. *In* Morton, J.L., Zierenberg, R.A., and Reiss, C.A. (Eds.), *Geologic, Hydrothermal, and Biologic Studies at Escanaba Trough, Gorda Ridge, Offshore Northern California*. U.S. Geol. Surv. Bull., 2022:65–75.

Duckworth, R.C., Fallick, A.E., and Rickard, D., 1994. Mineralogy and sulfur isotopic composition of the Middle Valley massive sulfide deposit, northern Juan de Fuca Ridge. *In* Mottl, M.J., Davis, E.E., Fisher, A.T., and Slack, J.F. (Eds.), *Proc. ODP, Sci. Results,* 139: College Station, TX (Ocean Drilling Program), 373–385.

Edmond, J.M., and Von Damm, K., 1983. Hot springs on the ocean floor. *Sci. Am.,* 248:78–84.

Elderfield, H., and Schultz, A., 1996. Mid-ocean ridge hydrothermal fluxes and the chemical composition of the ocean. *Annu. Rev. Earth Planet. Sci.,* 24:191–224.

Fisher, A.T., Becker, K., and Davis, E.E., 1997. The permeability of young oceanic crust east of Juan de Fuca Ridge determined using borehole thermal measurements. *Geophys. Res. Lett.,* 24:1311–1314.

Fouquet, Y., Zierenberg, R.A., Miller, D.J., et al., 1998. *Proc. ODP, Init. Repts.,* 169: College Station, TX (Ocean Drilling Program).

Glenn, S., 1998. One dimensional fluid flow modeling of the area of active venting, Middle Valley, northern Juan de Fuca Ridge [M.S. thesis]. Duke Univ., Durham, NC.

Goodfellow, W.D., and Franklin, J.M., 1993. Geology, mineralogy and chemistry of sediment-hosted clastic massive sulfides in shallow cores, Middle Valley, northern Juan de Fuca Ridge. *Econ. Geol.,* 88:2033–2064.

Goodfellow, W.D., Grapes, K., Cameron, B., and Franklin, J.M., 1993. Hydrothermal alteration associated with massive sulfide deposits, Middle Valley, Northern Juan de Fuca Ridge. *Can. Mineral.,* 31:1025–1060.

Goodfellow, W.D., and Peter, J.M., 1994. Geochemistry of hydrothermally altered sediment, Middle Valley, northern Juan de Fuca Ridge. *In* Mottl, M.J., Davis, E.E., Fisher, A.T., and Slack, J.F. (Eds.), *Proc. ODP, Sci. Results,* 139: College Station, TX (Ocean Drilling Program), 207–289.

Hannington, M.D., Jonasson, I.R., Herzig, P.M., and Petersen, S., 1995. Physical, chemical processes of seafloor mineralization at mid-ocean ridges. *In* Humphris, S.E., Zierenberg, R.A., Mullineaux, L.S., and Thomson, R.E. (Eds.), *Seafloor Hydrothermal Systems: Physical, Chemical, Biological and Geological Interactions*. Geophys. Monogr., Am. Geophys. Union, 91:115–157.

James, R.H., and Palmer, M.R., 1999. The alkali element and boron geochemistry of the Escanaba Trough sediment-hosted hydrothermal system. *Earth Planet. Sci. Lett.,* 171:157–169.

Janecky, D.R., and Seyfried, W.E., 1984. Formation of massive sulfide deposits on oceanic ridge crests: incremental reaction models for mixing between hydrothermal solutions and seawater. *Geochim. Cosmochim. Acta,* 48:2723–2738.

Karlin, R., and Lyle, M., 1986. Sediment studies on the Gorda Ridge. *Open File Rep.—Oreg. Dep. Geol. Miner. Ind.,* O-86-19.

Karlin, R.E., and Zierenberg, R.A., 1994. Sedimentation and neotectonism in the SESCA area, Escanaba Trough, southern Gorda Ridge. *In* Morton, J.L., Zierenberg, R.A., and Reiss, C.A. (Eds.), *Geologic, Hydrothermal, and Biologic Studies at Escanaba Trough, Gorda Ridge, Offshore Northern California*. U.S. Geol. Surv. Bull. 2022:131–142.

Koski, R.A., Benninger, L.M., Zierenberg, R.A., and Jonasson, I.R., 1994. Composition and growth history of hydrothermal deposits in Escanaba Trough, Southern Gorda Ridge. *In* Morton, J.L., Zierenberg, R.A., and Reiss, C.A. (Eds.), *Geologic, Hydrothermal, and Biologic Studies at Escanaba Trough, Gorda Ridge, Offshore Northern California*. U.S. Geol. Surv. Bull., 2022:293–324.

Krasnov, S., Stepanova, T., and Stepanov, M., 1994. Chemical composition and formation of a massive sulfide deposit, Middle Valley, northern Juan de Fuca Ridge (Site 856). *In* Mottl, M.J., Davis, E.E., Fisher, A.T., and Slack, J.F. (Eds.), *Proc. ODP, Sci. Results,* 139: College Station, TX (Ocean Drilling Program), 353–372.

Lackschewitz, K.S., Singer, A., Botz, R., Garbe-Schönberg, D., Stoffers, P., and Horz, K., 2000. Formation and transformation of clay minerals in the hydrothermal deposits of Middle Valley, Juan de Fuca Ridge, ODP Leg 169. *Econ. Geol.*, 95:361–390.

Morton, J.L., and Fox, C.G., 1994. Structural setting and interaction of volcanism and sedimentation at Escanaba Trough: geophysical results. *In* Morton, J.L., Zierenberg, R.A., and Reiss, C.A. (Eds.), *Geologic, Hydrothermal, and Biologic Studies at Escanaba Trough, Gorda Ridge, Offshore Northern California*. U.S. Geol. Surv. Bull., 2022:21–43.

Morton, J.L., Zierenberg, R.A., and Reiss, C.A., 1994. Geologic, hydrothermal, and biologic studies at Escanada Trough: An introduction. *In* Morton, J.L., Zierenberg, R.A., and Reiss, C.A. (Eds.). *U.S. Geol. Survey Bull.* 2022:1–18.

Mottl, M.J., Davis, E.E., Fisher, A.T., and Slack, J.F. (Eds.), 1994. *Proc. ODP, Sci. Results,* 139: College Station, TX (Ocean Drilling Program).

Mottl, M.J., Wheat, C.G., and Boulegue, J., 1994. Timing of ore deposition and sill intrusion at Site 856: evidence from stratigraphy, alteration, and sediment pore-water composition. *In* Mottl, M.J., Davis, E.E., Fisher, A.T., and Slack, J.F. (Eds.), *Proc. ODP, Sci. Results,* 139: College Station, TX (Ocean Drilling Program), 679–693.

Normark, W.R., Gutmacher, C.E., Zierenberg, R.A., Wong, F.L., and Rosenbauer, R.J., 1994. Sediment fill of Escanaba Trough. *In* Morton, J.L., Zierenberg, R.A., and Reiss, C.A. (Eds.), *Geologic, Hydrothermal, and Biologic Studies at Escanaba Trough, Gorda Ridge, Offshore Northern California*. U.S. Geol. Surv. Bull., 2022:91–130.

Rigsby, C.A., Zierenberg, R.A., and Baker, P.A., 1994. Sedimentary and diagenetic structures and textures in turbiditic and hemiturbiditic strata as revealed by whole-core X-radiography, Middle Valley, northern Juan de Fuca Ridge. *In* Mottl, M.J., Davis, E.E., Fisher, A.T., and Slack, J.F. (Eds.), *Proc. ODP, Sci. Results,* 139: College Station, TX (Ocean Drilling Program), 105–111.

Rohr, K.M.M., and Schmidt, U., 1994. Seismic structure of Middle Valley near Sites 855–858, Leg 139, Juan de Fuca Ridge. *In* Mottl, M.J., Davis, E.E., Fisher, A.T., and Slack, J.F. (Eds.), *Proc. ODP, Sci. Results,* 139: College Station, TX (Ocean Drilling Program), 3–17.

Ross, S.L., Klitgord, K.D., Reid, J.A., and Zierenberg, R.A., 1996. Recent sidescan imagery of NESCA site at Escanaba Trough, southern Gorda Ridge. *Eos,* 77:F316.

Schultheiss, P.J., 1997. Advances in fluid flow determinations for marine hydrogeology using pore pressure measurements. *Eos,* 78:672.

Stein, J.S., and Fisher, A.T., in press. Multiple scale hydrothermal circulation in Middle Valley, northern Juan de Fuca Ridge: physical constraints and geologic models. *J. Geophys. Res.*

Stein, J.S., Fisher, A.T., Langseth, M., Jin, W., Iturrino, G., and Davis, E., 1998. Fine-scale heat flow, shallow heat sources, and decoupled circulation systems at two sea-floor hydrothermal sites, Middle Valley, northern Juan de Fuca Ridge. *Geology,* 26:1115–1118.

Tivey, M.A., 1994. High-resolution magnetic surveys over the Middle Valley mounds, northern Juan de Fuca Ridge. *In* Mottl, M.J., Davis, E.E., Fisher, A.T., and Slack, J.F. (Eds.), *Proc. ODP, Sci. Results,* 139: College Station, TX (Ocean Drilling Program), 29–35.

Turner, R.J.W., Ames, D.E., Franklin, J.M., Goodfellow, W.D., Leitch, C.H.B., and Hoy, T., 1993. Character of hydrothermal mounds and nearby altered hemipelagic sediments in the hydrothermal areas of Middle valley, northern Juan de Fuca Ridge: shallow core data. *Can. Mineral.,* 31:973–995.

Urbat, M., Dekkers, M.J., and Kramsiek, K., 2000. Discharge of hydrothermal fluids through sediment at Escanaba Trough, Gorda Ridge (ODP Leg 169): assessing the effects on rock magnetic signal. *Earth Planet. Sci. Lett.* 176: 481–494.

Vallier, T.L., Harold, P.J., and Girdley, W.A., 1973. Provenances and dispersal patterns of turbidite sand in Escanaba Trough, northeastern Pacific Ocean. *Mar. Geol.,* 1:67–87.

Zierenberg, R.A., Fouquet, Y., Miller, D.J., Bahr, J.M., Baker, P.A., et al., 1998. The deep structure of a sea-floor hydrothermal deposit. *Nature* 392:485–488.

Zierenberg, R.A., Koski, R.A., Morton, J.L., Bouse, R.M., and Shanks, W.C., III, 1993. Genesis of massive sulfide deposits on a sediment-covered spreading center, Escanaba Trough, 41°N, Gorda Ridge. *Econ. Geol.,* 88:2069–2098.

Zierenberg, R.A., Morton, J.L., Koski, R.A., and Ross, S.L., 1994. Geologic setting of massive sulfide mineralization in the Escanaba Trough. *In* Morton, J.L., Zierenberg, R.A., and Reiss, C.A. (Eds.), *Geologic, Hydrothermal, and Biologic Studies at Escanaba Trough, Gorda Ridge, Offshore Northern California*. U.S. Geol. Surv. Bull., 2022:171–197.

Zuffa, G.G., Normark, W.R., Serra, F., and Brunner, C.A., 2000. Turbidite megabeds in an oceanic rift valley recording jökulhaups of late Pleistocene glacial lakes of the western United States. *Journal of Geology*, 108:253-274.

Figure F1. Location map showing tectonic setting of the sediment-covered spreading centers at Middle Valley and Escanaba Trough on the Juan de Fuca–Gorda Ridge spreading system.

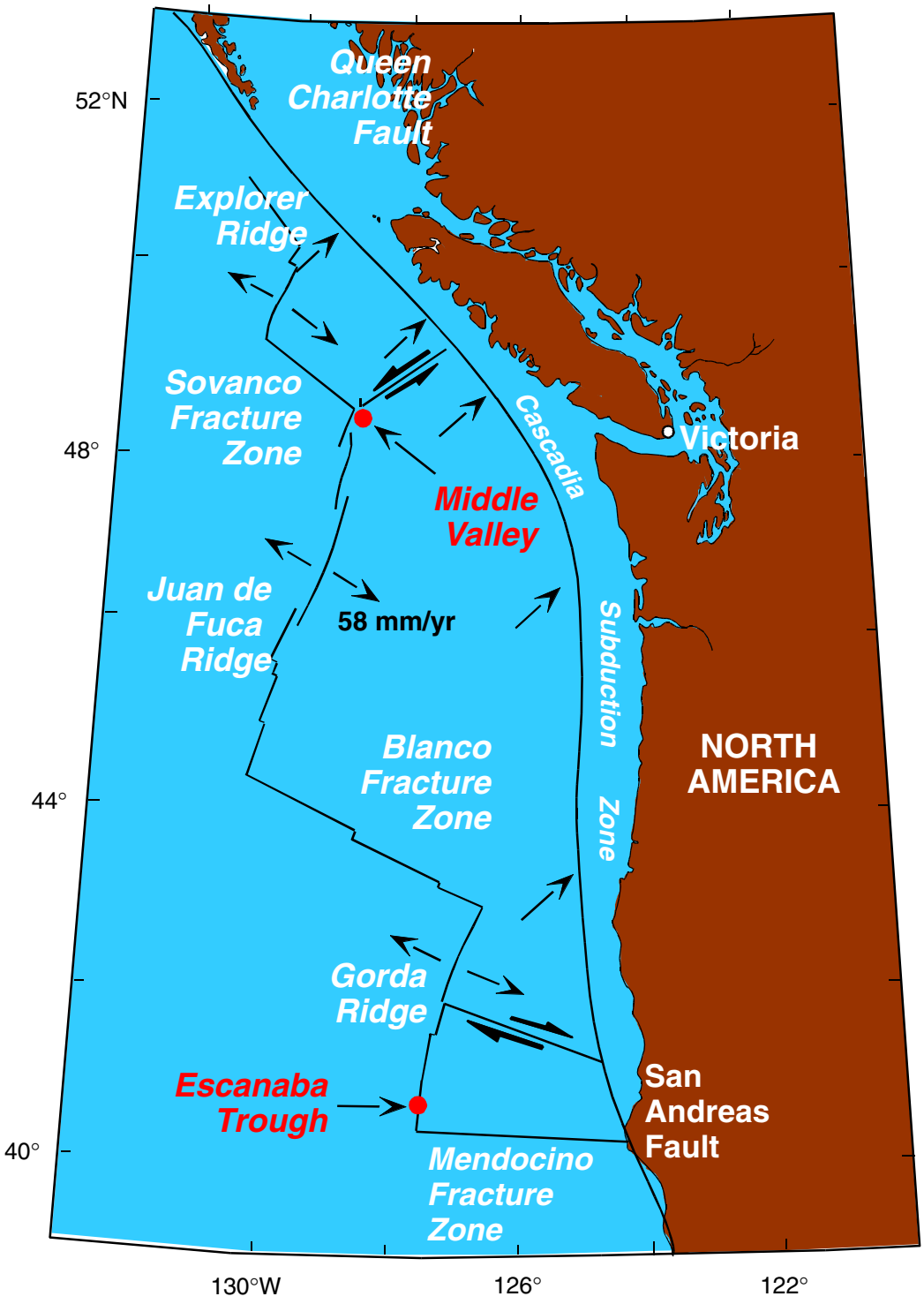

Figure F2. Bathymetry of Middle Valley shown as contours drawn at 20-m intervals. The locations of Dead Dog vent field in the area of active venting (Sites 858 and 1036) and Bent Hill (Sites 856 and 1035) are noted. Modified from Davis et al. (1987).

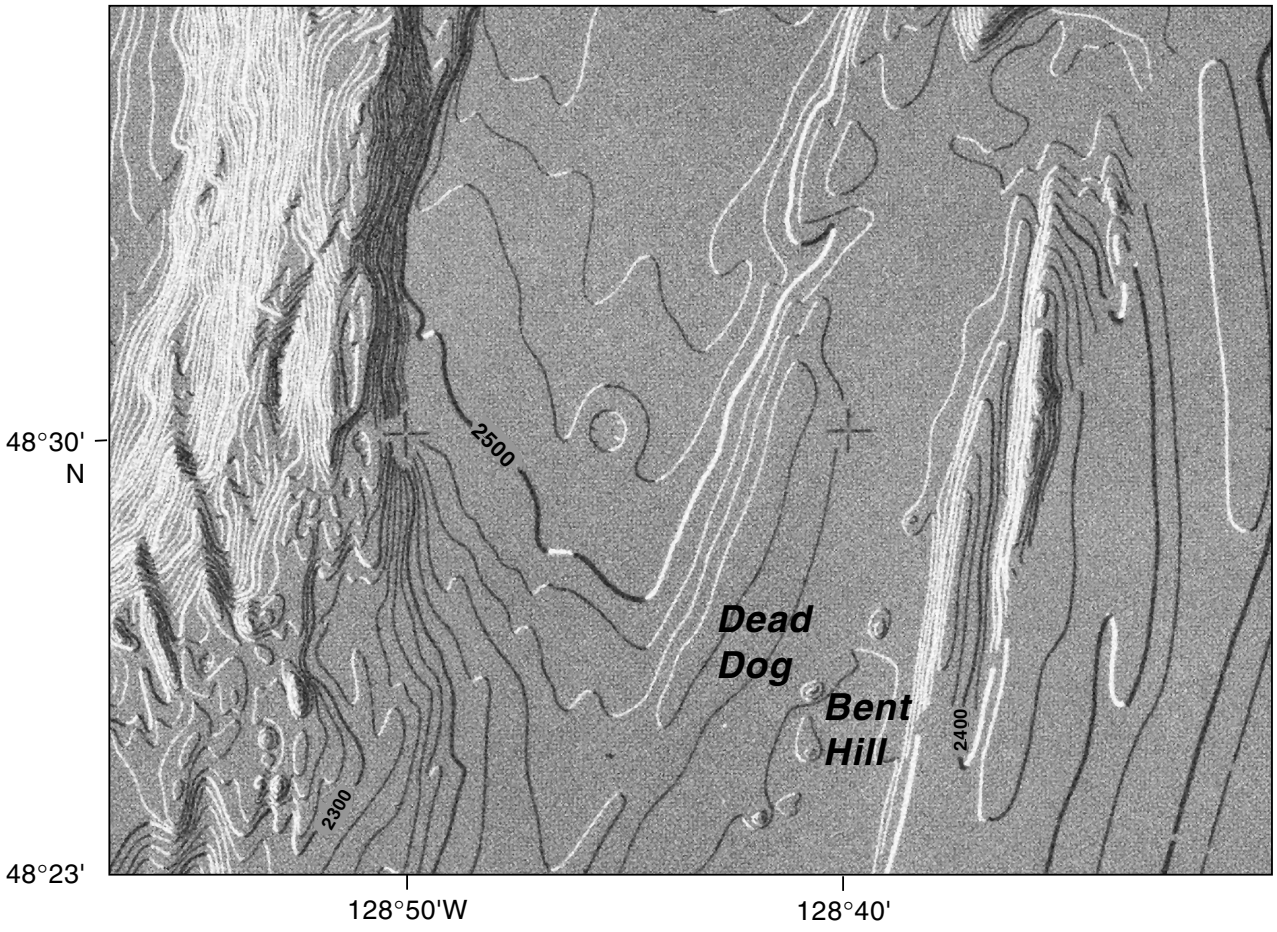

Figure F3. Map of Bent Hill (Middle Valley area) showing the location of Bent Hill and the two massive sulfide mounds (Bent Hill and ODP Mound massive sulfide deposits) to the south. The positions of holes drilled during Leg 139 (open circles) and Leg 169 (solid circles) are shown. Modified from Goodfellow and Peter (1994).

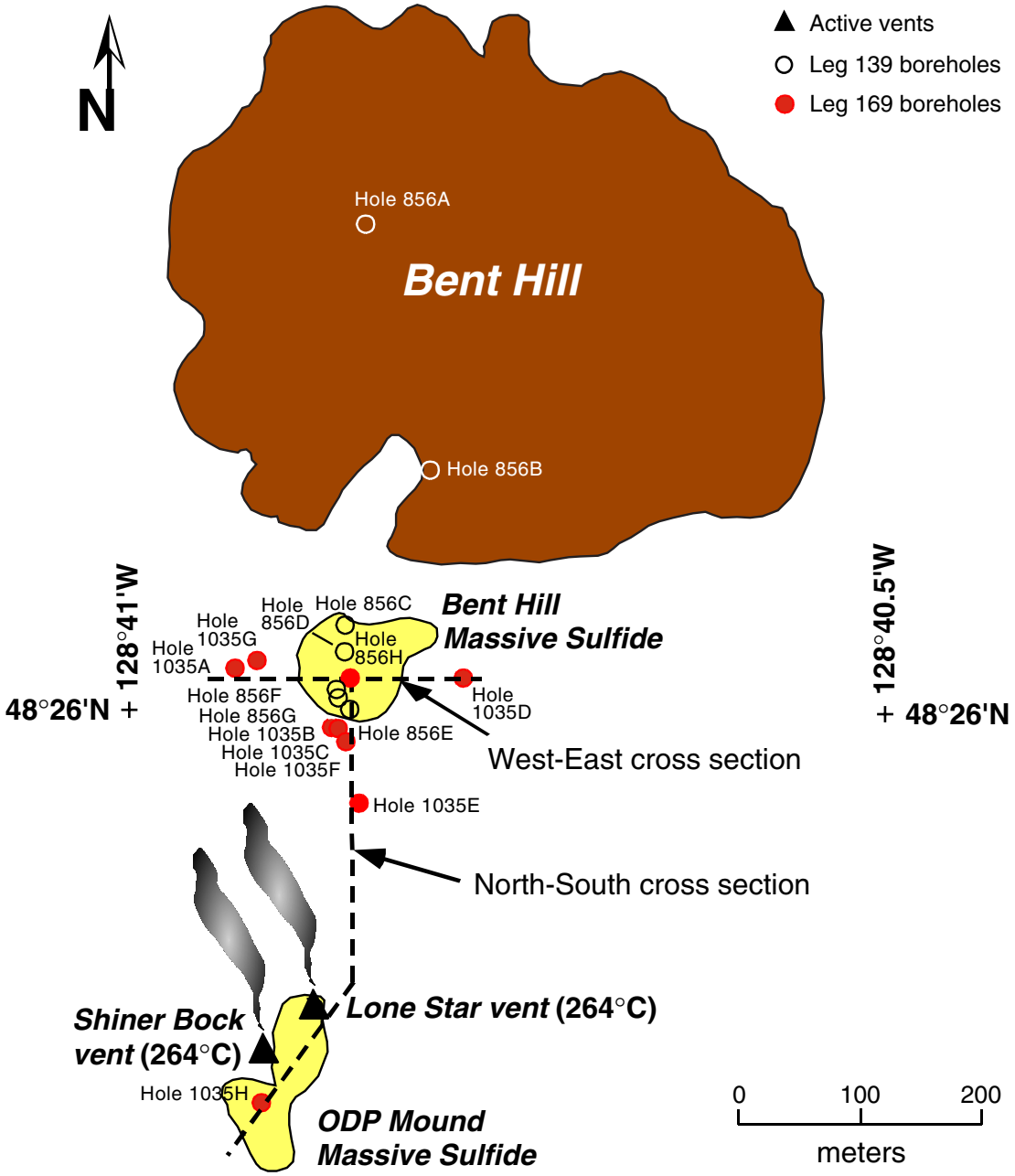

Figure F4. Map of Dead Dog vent field (Middle Valley area) showing the location of the major hydrothermal mounds, active vents, and the holes drilled during Leg 139 (open circles) and Leg 169 (solid circles). The limit of the vent field was determined as the contour of the acoustic sidescan sonar reflector. Modified from Butterfield et al. (1994).

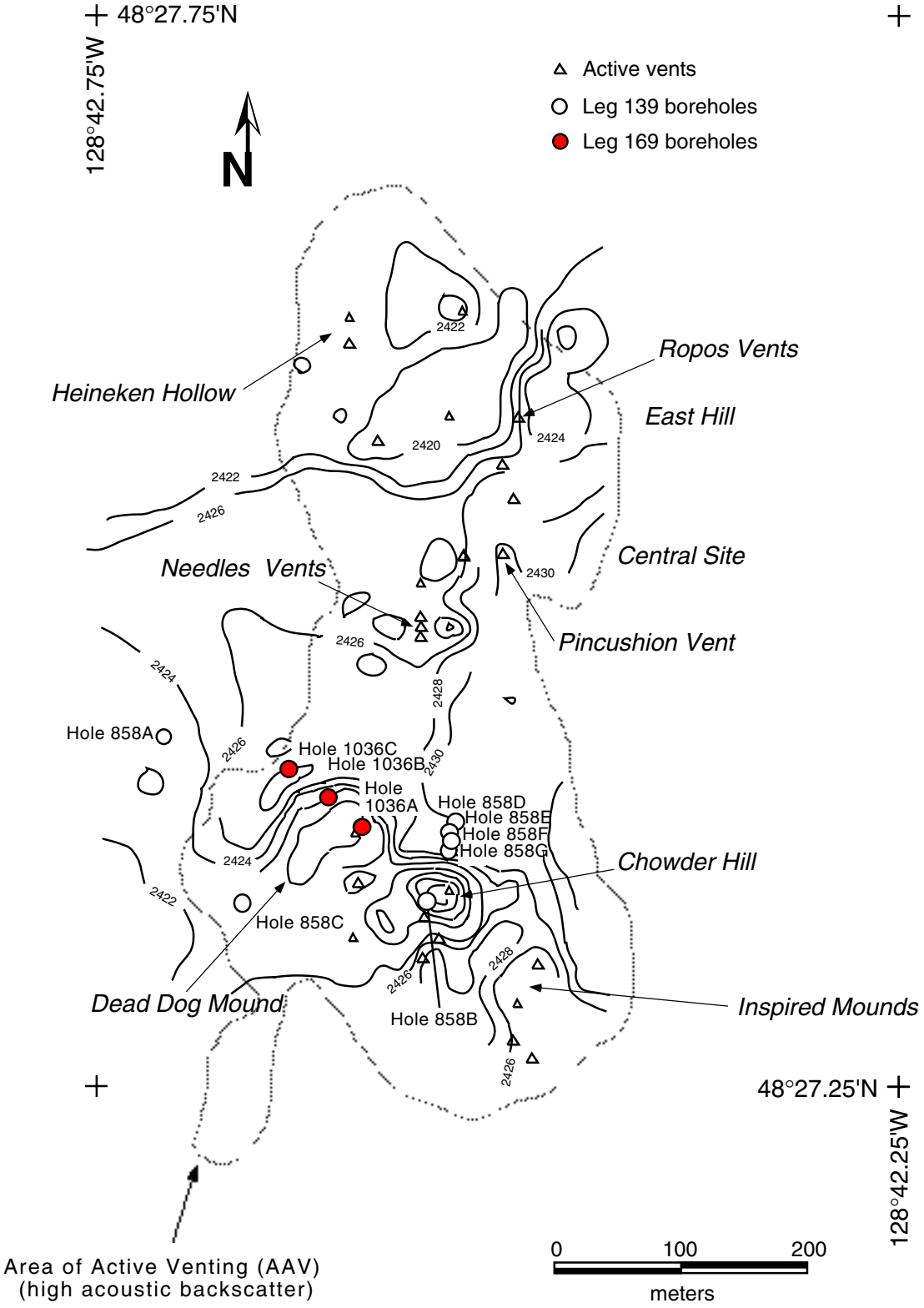

Figure F5. Map of Escanaba Trough in the southern portion of the Gorda Ridge spreading center showing the sediment-filled portion of the trough, intratrough terraces, and the volcanic centers that rise through and locally pierce the sediment cover. The location of Sites 1037 (reference hole) and 1038 drilled during Leg 169 are shown. NESCA = northern Escanaba Trough study area and SESCA = southern Escanaba Trough study area. Modified from Morton et al., 1994.

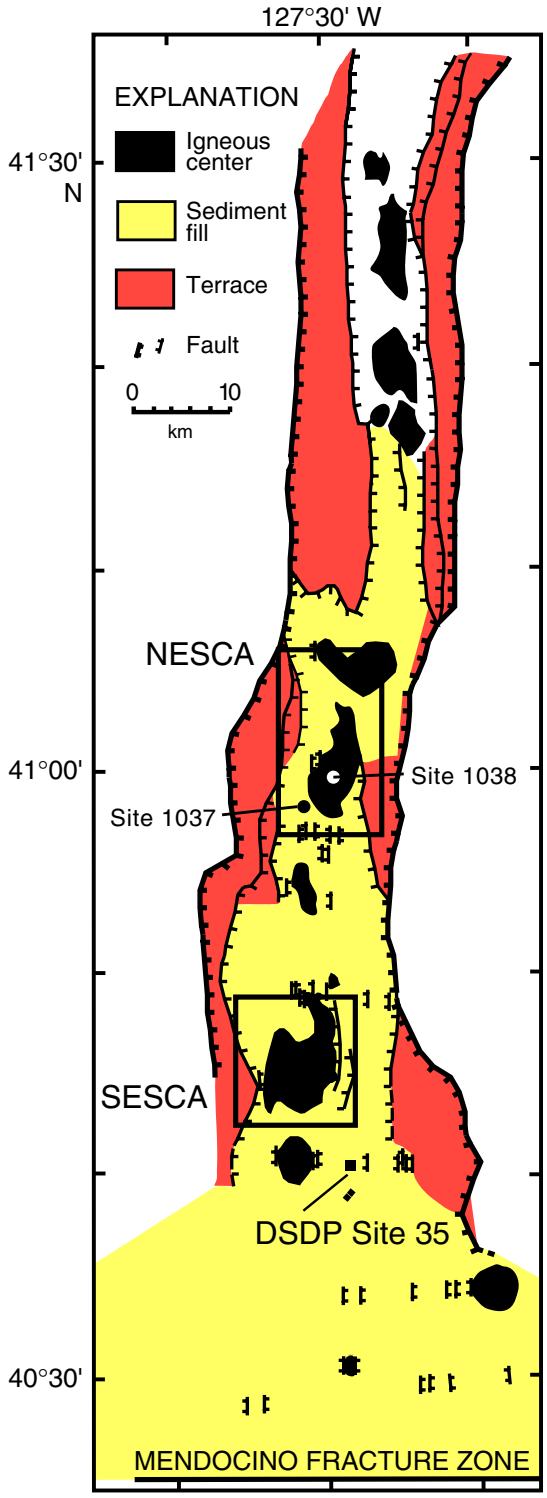

Figure F6. Detailed map of Central Hill showing the position of holes drilled at Site 1038 during Leg 169. Location of active vents and exposed volcanic rock are based on camera tows and submersible tracks shown as thin lines. Modified from Zierenberg et al., 1994.

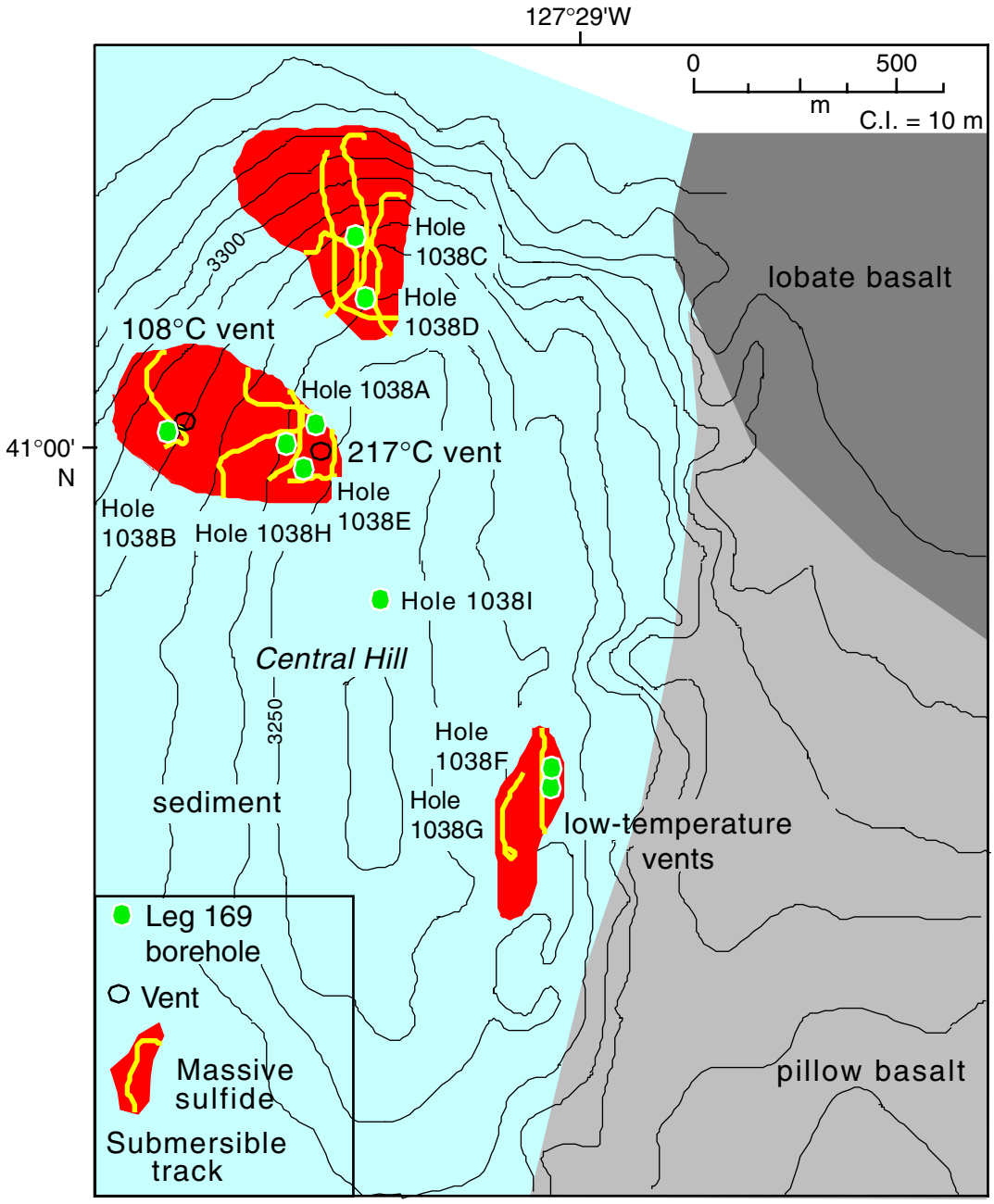

Figure F7. North-south cross section of the BHMS deposit and ODP Mound, the underlying feeder zones, the Deep Copper Zone, host turbiditic and hemipelagic sedimentary rocks, and underlying basaltic sills and flows. Modified from Zierenberg et al., 1998.

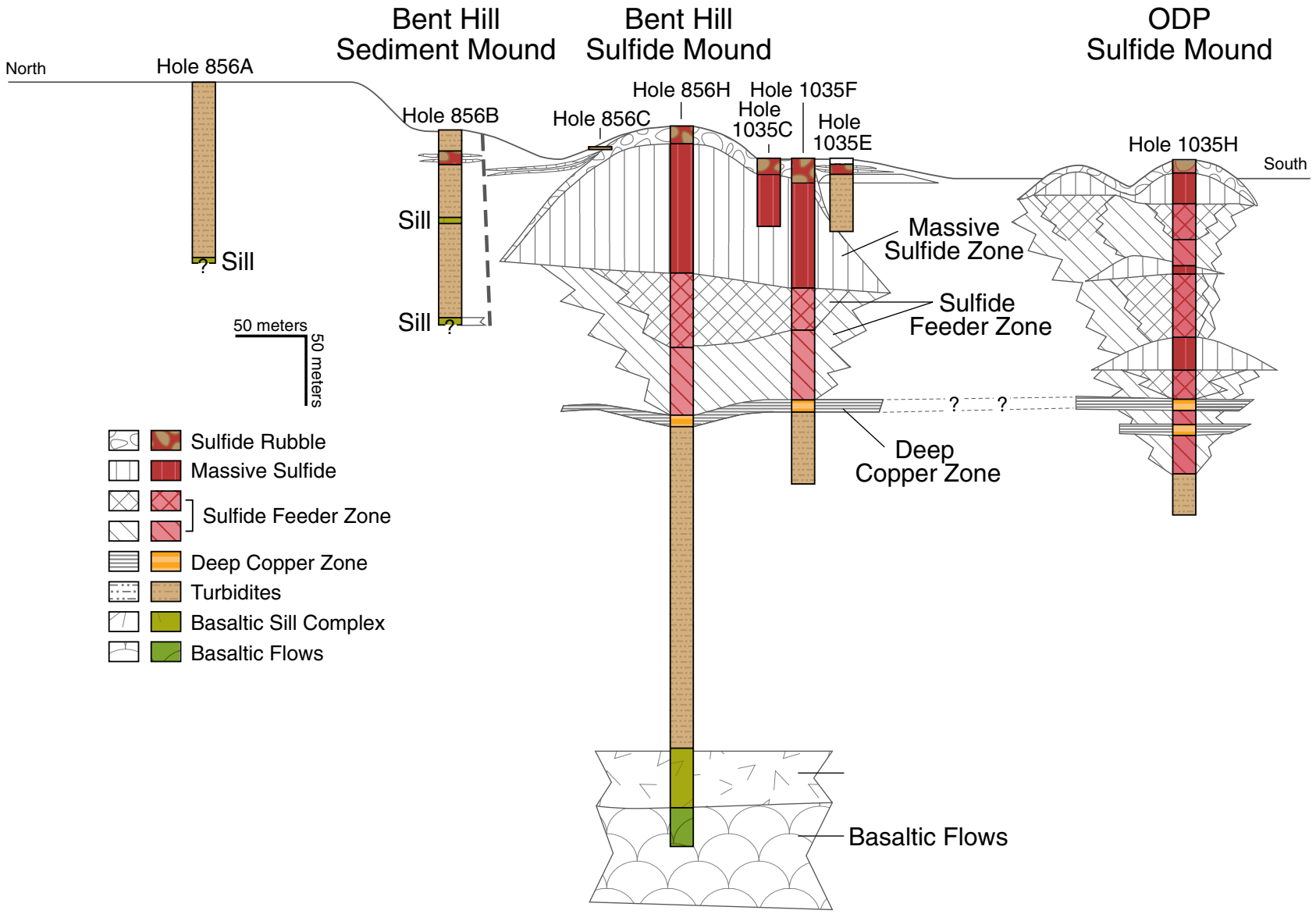

Figure F8. Subvertical single and multiple massive sulfide veins composed of pyrrhotite, isocubanite, pyrite, magnetite, and anhydrite cutting hydrothermally altered and lithified sediment from the feeder zone beneath the BHMS deposit (Section 169-856H-24R-1).

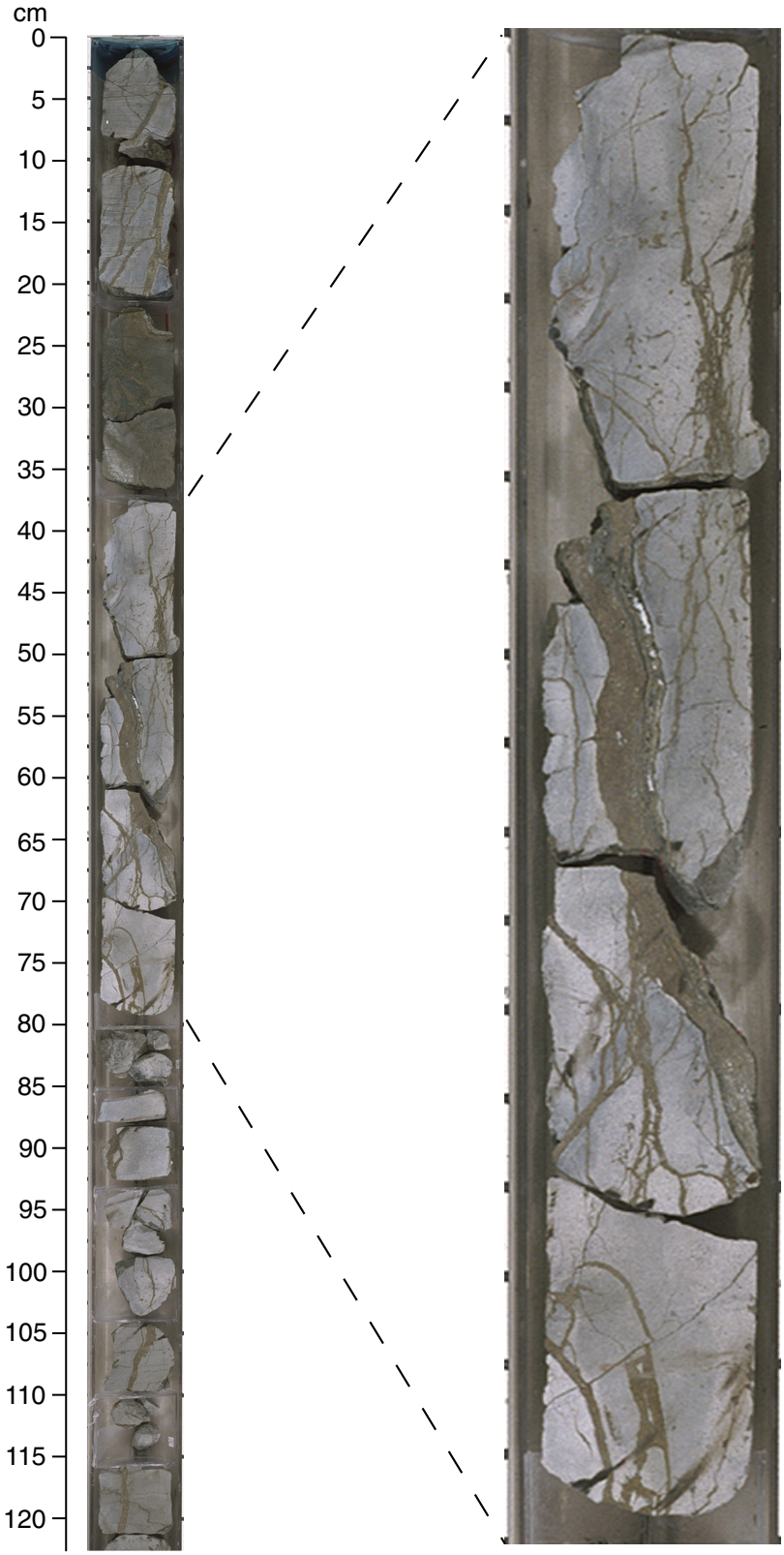

Figure F9. Composite chalcopyrite, isocubanite, pyrite, pyrrhotite vein formed by coalescing of thin veins and some crack-seal vein formation (interval 169-856H-21R-1, 90–108 cm).

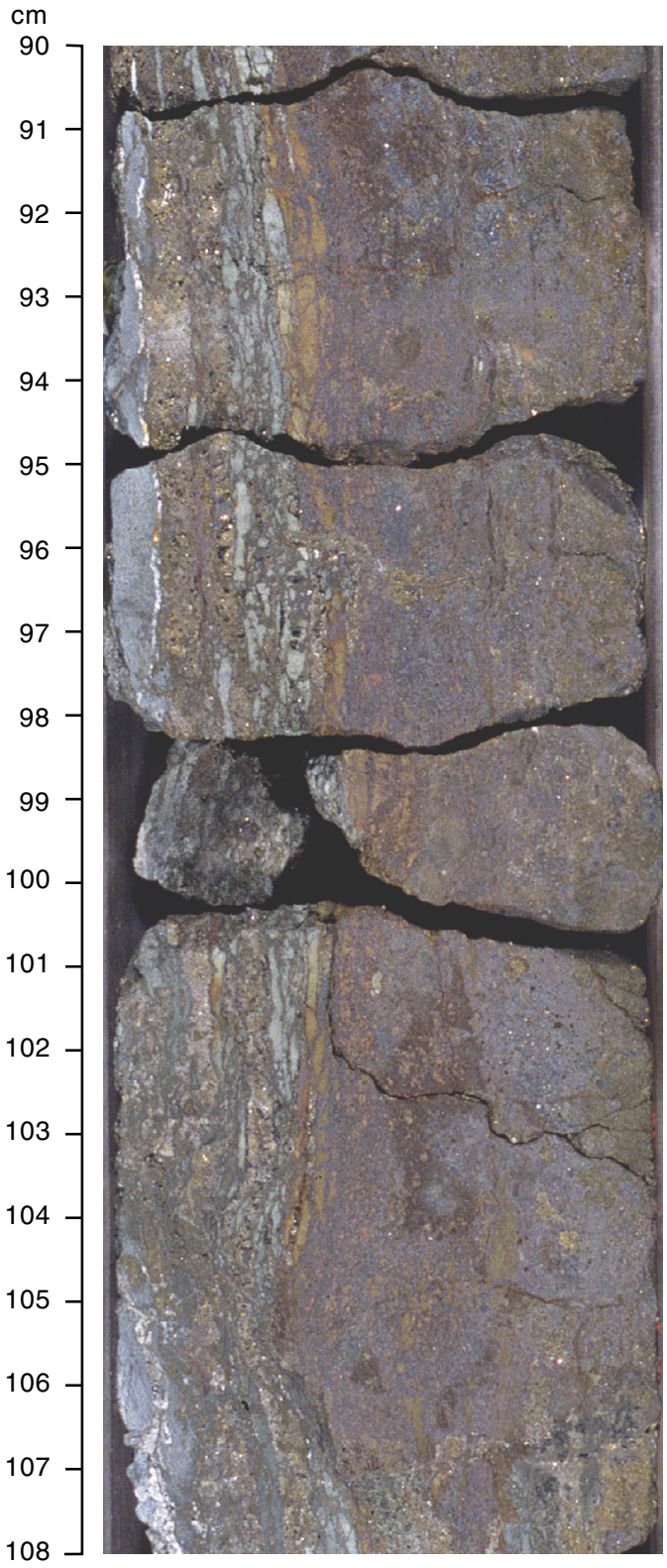

Figure F10. Sulfide-banded, cross-laminated sandstone. Horizontal development of Cu-rich sulfide mimics sedimentary structures and replaces sandstone. Note the absence of vertical veins (interval 169-856H-31R-1, 99–106 cm).

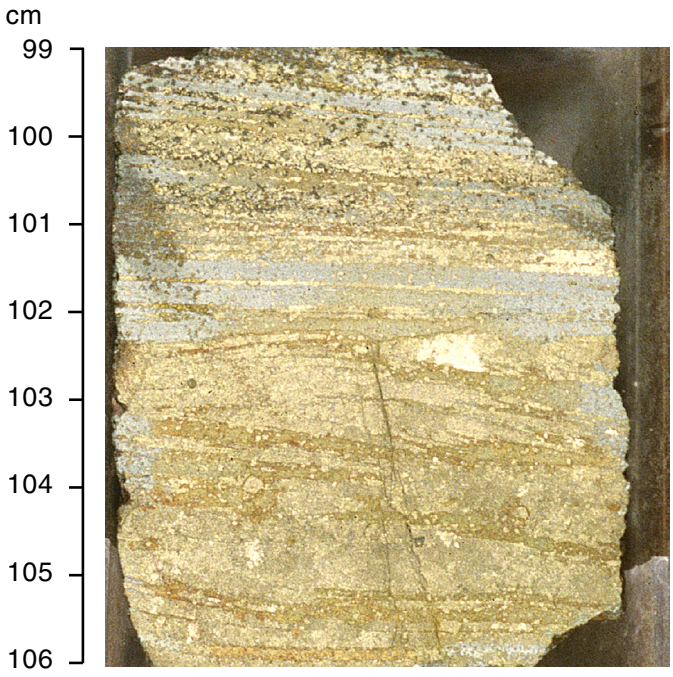

Figure F11. Diagram showing the depth to basement in the two Middle Valley holes that were reinstrumented with CORKs. Basement (shaded areas) at Site 857 is defined as the top of a sill-sediment complex at 470 mbsf. Basement rises to 250 mbsf under Site 858 and is extrusive basalt (from Davis and Becker, 1994a).